

EVOLUTION OF THE EAST ANTARCTIC ICE SHEET: A RECORD FROM THE
SEISMIC STRATIGRAPHY OF THE C-19 SITE, ROSS SEA, ANTARCTICA

Howard Preston Viator III

A thesis submitted to the faculty of the University of North Carolina at Chapel Hill in partial fulfillment of the requirements for the degree of Master of Science in the Department of Geological Sciences.

Chapel Hill
2009

Approved by:

Dr. Louis R. Bartek, III

Dr. Joseph Carter

Dr. Stephen Meyers

ABSTRACT

HOWARD PRESTON VIATOR III: Evolution of the East Antarctic Ice Sheet: A Record
from the Seismic Stratigraphy of the Ross Sea, Antarctica
(Under the direction of Dr. Louis R. Bartek, III)

Nearly 1000 km of high-resolution single-channel seismic (SCS) reflection data and 1000 km of multi-channel seismic (MCS) data were acquired in the Ross Sea, Antarctica where a large iceberg, C-19, calved from the Ross Ice Shelf in May of 2002. This data set offers a unique opportunity to use a closely spaced grid of high-resolution seismic profiles to examine the glacial history of the continental shelf in an up-dip location, where older strata are closer to the surface. Two major grounding events are evident in the stratigraphic record; the first one representing the initial advance of ice onto the continental shelf during the early Miocene. During the Oligocene, prior to the onset of widespread glaciation from the East Antarctic Ice Shelf on the continental shelf, this area experienced multiple cycles (at least 10) of ice sheet advance/retreat representing an ice sheet that is approaching but not reaching the C-19 site.

ACKNOWLEDGEMENTS

I would like to thank Dr. Louis R. Bartek III, and my committee members Dr. Joseph Carter and Dr. Stephen Myers for their insight and time.

I would like to thank the National Science Foundation, grant #OPP-0087392, for funding this research. I would also like to thank the students and faculty from UNC-Chapel Hill and UC Santa Barbara for help with the collection this data set.

And, of course, my wonderful friend and family for their support and encouragement.

TABLE OF CONTENTS

LIST OF TABLES	vi
LIST OF FIGURES	vii
LIST OF ABBREVIATIONS	ix
Chapter	
1. INTRODUCTION	1
1.1 Regional Setting.....	1
1.2 Previous Work	3
1.3 Project Overview	8
1.4 Project Goals.....	11
1.4.1 Glacial History.....	11
1.4.2. MCS Aliasing.....	12
2. METHODS	14
2.1 Data acquisition and processing	14
2.2 Seismic stratigraphic analyses	15
2.3 Maps	19
2.4 MCS Aliasing	20
3. RESULTS	21
3.1 Seismic stratigraphy	21
3.2 MCS Aliasing.....	32
4. DISCUSSION	42

4.1 Chronostratigraphy	42
4.2 Sequence interpretations	42
4.3 EAIS Evolution	52
4.4 MCS Aliasing	55
5. CONCLUSIONS	56
REFERENCES	58

LIST OF TABLES

Table

2.1	Seismic facies criteria	19
3.1	MCS alias table	41

LIST OF FIGURES

Figure

1.1	Map of Antarctica	2
1.2	Regional map showing study area and correlation path	10
1.3	Map showing C-19 tracklines	11
2.1	Seismic termination patterns.....	16
2.2	Seismic facies standards	17
2.3	Seismic facies standards	18
3.1	Unit RSS-2 isochron map	22
3.2	Seismic example of erosional unconformity.....	23
3.3	Seismic example of erosional unconformity.....	24
3.4	Seismic example of angular unconformity	26
3.5	Unit RSS-3 isochron map	27
3.6	Seismic example of minimal internal reflections.....	28
3.7	Seismic example of minimal internal reflections.....	29
3.8	Seismic example of cross-cutting reflections (RSS-3)	30
3.9	Facies isochron map unit RSS-3	31
3.10	Unit RSS-4 isochron map	33
3.11	Seismic example of minimal internal reflections.....	34
3.12	Seismic example of cross-cutting reflections (RSS-4)	35
3.13	Seismic example of cross-cutting reflection (RSS-4).....	36
3.14	Facies isochron map unit RSS-4	37
3.15	Seismic example of SCS – MCS comparison.....	39

3.16	Seismic example of SCS – MCS comparison.....	40
4.1	Illustration of glacial-marine depositional process	45
4.2	Illustration of open marine depositional process	46
4.3	Illustration of sub-glacial depositional process.....	49
4.4	Facies distribution map (RSS-3).....	50
4.5	Facies distribution map (RSS-4).....	51
4.6	Seismic example of cross-cutting reflections (RSS-3 and RSS-4)	53

LIST OF ABBREVIATIONS

EAIS	East Antarctic Ice Sheet
MCS	Multi-channel seismic
MS	Millisecond
SCS	Single-channel seismic
TWT	Two-way-travel time

CHAPTER 1

INTRODUCTION

1.1 Regional Setting

Modern Antarctica supports an ice cap of nearly 30,000,000 km³, representing 90% of Earth's ice volume (Denton et al., 1991). This ice is located mostly in the two major ice sheets of Antarctica, the West Antarctic Ice Sheet (WAIS) and the East Antarctic Ice Sheet (EAIS) (Figure 1.1). If Antarctica's ice sheets completely melted, there would be an influx of fresh water into the oceans large enough to raise worldwide sea level by approximately 70 m (Sahagian, 1987). At the peak of the last glacial maximum, the Antarctic Ice Sheet contained a volume of ice equivalent to ~95 m of sea-level change (Hughes et al, 1981).

An atypical example of a continental shelf lies beneath the Ross Sea. Extension and subsidence lead to the formation of three north-south trending sedimentary basins, the Victoria Land basin, the Central Trough and the Eastern Basin (Davey et al, 1982), with sediment thicknesses ranging from 8 to 14 km. The Ross Embayment generally shallows toward the shelf break from 500-1000 m beneath the ice shelf to less than 300 m near the shelf edge. This odd shelf morphology is due to the processes of overdeepening - depression of the lithosphere due to the weight of the Antarctic Ice Sheets - and foredeepening - the redistribution of sediment from the inner shelf to the outer shelf via glacial activity (Holtedahl, 1929).

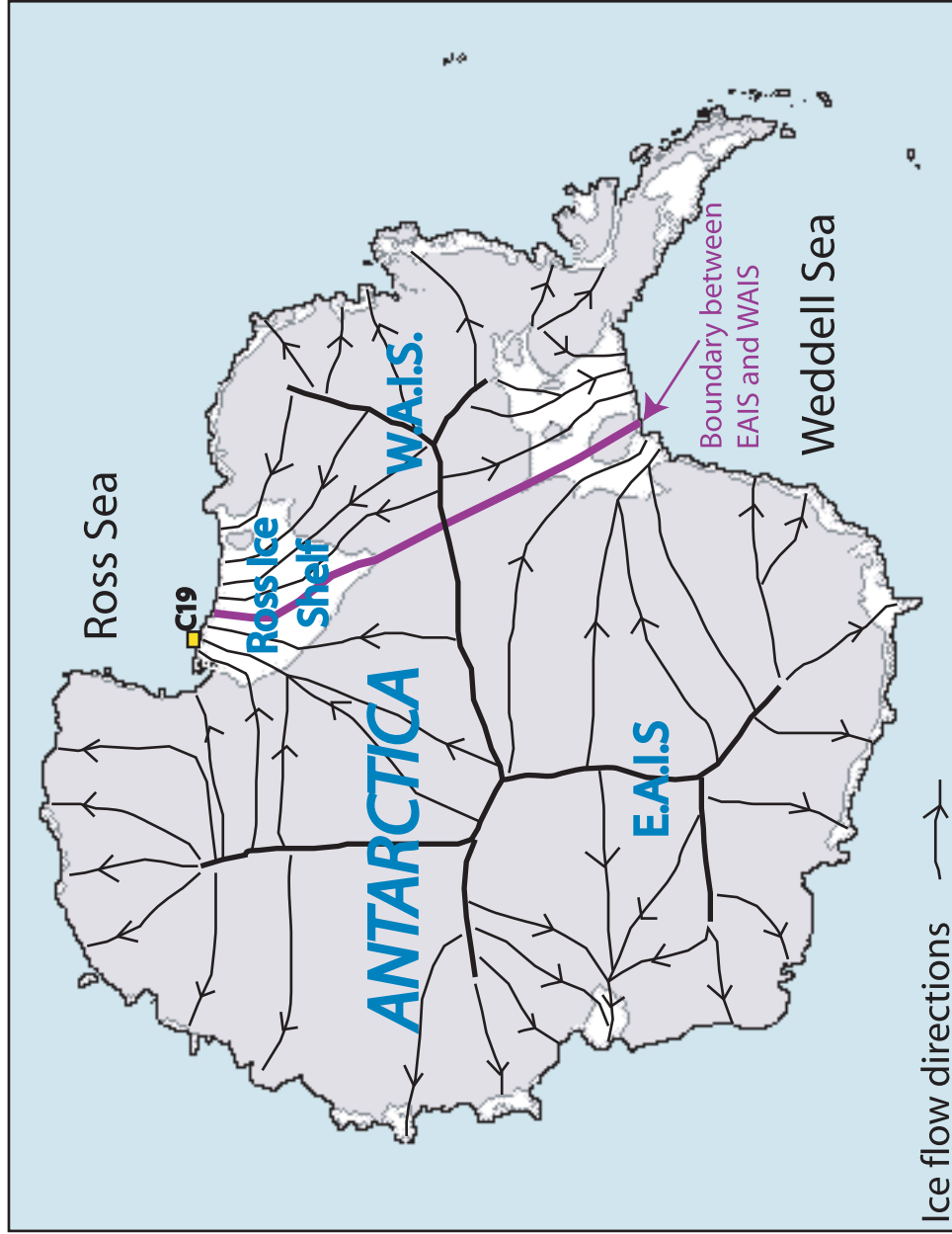


Figure 1.1 - Map of Antarctica showing C-19 study area, major ice sheets and ice drainage paths (black arrows).

The bulk of Antarctica's ice is retained in the EAIS, a land based ice sheet with two major outlets into the Southern Ocean; the Amery Ice Shelf in Prydz Bay and the Ross Ice Shelf in the Ross Sea. Twenty-five percent of the volume of the Antarctic ice sheets feeds into the Ross Ice Shelf (Bartek et al., 1997), which makes the Ross Sea a prime testing area for models on the history of Antarctic ice sheet fluctuations.

1.2 Previous Work

There have been a number of attempts to reconstruct the evolution of the EAIS by interpreting events seen in proxy records as volume fluctuations of the EAIS. These proxies include records of ice-rafted debris (IRD) (Hayes et al., 1975; Hambrey and Barrett, 1993), oxygen isotope studies (Miller et al., 2005; Shackleton and Kennett, 1975) as well as terrestrial deposits (Harwood and Webb, 1998; Stroeve et al., 1998). IRD offers only an inferred link to ice sheet size due to uncertainties about the mechanisms of iceberg calving events. While isotope studies produce temperature and ice volume reconstructions, they do not offer direct evidence of fluctuations in Antarctic ice sheet volume. Consequently, it is unknown how well the variations seen in these records correlate with variations in the extent of the EAIS.

A number of drill sites scattered throughout the Ross Sea provide evidence for past glacial advances. In 1973, the Deep Sea Drilling Project (DSDP) Leg 28 drilled four sites, 270, 271, 272 and 273, on the central Ross Sea continental shelf. The CIROS-1 (Cenozoic Investigation of the Ross Sea) site, located 12 km off the coast in western McMurdo Sound was drilled in 1986 and achieved a total recovery of 98% (Hambrey et al., 1989). A third drilling project in the area is the Cape Roberts Project (CRP). The CRP sites, drilled in 1997

in western McMurdo Sound near Cape Roberts, achieved a recovery of 77%. These drill sites, accompanied by local and regional seismic stratigraphic interpretations as well as various oxygen isotope based sea-level reconstructions provide a base of evidence about past glacial events in the Ross Sea region, which is sometimes contradictory.

Oligocene

Some of the very first evidence discovered comes from sea-level reconstructions done in the 1980s. The sea-level curve constructed via seismic stratigraphy from various continental margins around the world by Haq et al. (1987) shows a substantial shallowing during the mid-Oligocene, which is interpreted to be a glacioeustatic response to Antarctic Ice Sheet formation. However, the oxygen isotope-based sea-level curve of Miller et al. (2005) indicates continental ice build-up in the earliest Oligocene, not the mid-Oligocene as indicated by Haq et al. (1987).

There are various lines of evidence for the existence of continental ice sheets on Antarctica, some claim the presence of ice all the way back in the late Cretaceous-early Eocene (Miller et al., 2005). Shackleton and Kennett (1975) noted from the deep-sea oxygen isotope record a major enrichment in ^{18}O in the earliest Oligocene and attributed this to ice buildup on Antarctica. Miller et al. (1991) noted a similar positive ^{18}O excursion in their reconstruction from subtropical planktonic foraminifera and dubbed this event Oi1 (circa 35.8 Ma), which was also interpreted to represent Antarctic ice build-up. These oxygen isotope studies seem to be in accord about the buildup of continental ice on Antarctica in the Oligocene, but offer no direct evidence of ice reaching the continental margin.

The first evidence for the occurrence of ice on the Antarctic continental margin comes from the appearance of IRD in the DSDP sites and indicates that the latest Oligocene saw ice reach the coast for the first time (Hayes et al., 1975). The lower sequence of the CIROS-1 drill core dates to the early Oligocene and is dominated by relatively deep water marine mudstones and sandstones with clasts scattered throughout that are interpreted to be IRD (Hambrey et al., 1989). Hambrey and Barrett (1993) interpret this as evidence that the glacier grounding line approached but did not cover the site; they speculate that early Oligocene conditions varied from limited tidewater glacier cover draining from the Transantarctic Mountains to an extended ice front beyond the confines of the mountains out onto the shelf. The data amassed from the drill sites in western McMurdo Sound provide definitive evidence of ice on the Antarctic coast, but do not confirm the first occurrence of a shelf-wide grounding event due to their proximity to the Transantarctic Mountains and the possibility that the sediments in the drill cores were deposited by simple valley glaciers instead of the ice sheet.

Oligocene – Miocene transition

Evidence for a grounded ice sheet on the continental shelf is much stronger by the late Oligocene-early Miocene. Anderson and Bartek (1992) identified evidence from their seismic stratigraphic analysis of strata of this age, including areas of the shelf that are deeply scoured by grounded ice sheets (resulting in foredeepened topography), glacial troughs and till tongues that is consistent with ice sheet expansion at this time. These findings are supported by discoveries by the Cape Roberts Science Team (1999) from the CRP drill site that indicate an expansion of the Antarctic Ice Sheet at the Oligocene-Miocene boundary,

possibly up to 20% larger than the present ice sheet (Naish et al., 2008). Investigation of the DSDP Leg 28 drill sites by Hayes et al. (1975) resulted in a similar claim, an unconformity of late Oligocene age (circa 25 Ma) indicating that major continental glaciation expanded on the shelf. Mi1 (circa 23.5 Ma), identified by Miller et al. (1991) is a positive ^{18}O excursion that also supports a massive buildup of ice at the Oligocene-Miocene boundary.

Despite these strong lines of evidence, questions remain about the nature of glaciation at this time. The first coring of the Oligocene-Miocene boundary in Antarctica is at DSDP site 270 in the Eastern Ross Sea (Hayes and Frakes, 1975). Massive diamictites recovered at the site date back to the late Oligocene-early Miocene, but it is unclear whether they represent subglacial or glacial-marine activity (Anderson and Bartek, 1992). Strata recovered from both CIROS-1 and the CRP sites reveal glacial advance and retreat cycles across the margin (Naish et al., 2001) but the nature of the ice remains unclear (i.e. local outlet glacier or shelf-wide ice sheet grounding events).

Miocene

IRD found in the DSDP cores suggest that by early to middle Miocene (22-10 Ma) the EAIS had grown large enough to breach the Transantarctic Mountains (Hayes et al., 1975). However, Bart (2003) offers the following lines of reasoning to suggest that the EAIS was not large enough to overtop the mountains even during the peak glaciations of the middle Miocene. First, the lithology of ice-rafted pebbles found at DSDP site 273 in the estimated age range of 15.7 to 14.4 Ma indicate that the provenance was probably somewhere in the West Antarctic interior basins (Barrett, 1975) as opposed to the Transantarctic Mountains. Second, progradation directions of grounding-zone till deltas on

the Ross Sea outer continental shelf are primarily basinward directed (toward the north) (Chow and Bart, 2003), rather than eastward directed as would be expected had the ice advanced from the mountains. Bart (2003) does propose, however, that the presence of ice-rafted diabase pebbles within the middle Miocene strata at DSDP site 272 suggest that the EAIS may have been sufficiently large sometime between 13.9 and 13.7 Ma to breach and/or overtop the Transantarctic Mountains, which is the only known source of diabase. He notes the possibility of outlet valley glaciers being the source of the pebbles. Other ambiguous evidence from IRD exists as well.

Hambrey and Barrett (1993) observed diatom-bearing mud with IRD in the middle Miocene sediments of DSDP site 273, and suggest a distal glacial-marine setting with limited ice cover. However, they also point out that equivalent strata at site 272 include proximal glacial-marine sediments and waterlain tills, implying extensive ice cover at that time.

Stratigraphic analysis by Anderson and Bartek (1992) reveals large troughs, similar in size to those carved by modern ice streams, in the early-middle Miocene seismic record, indicating that this was a time of major ice buildup in the Ross Sea region. They also point out that the middle Miocene unconformity seen in regional seismic lines and site 272 and 273 records an episode of ice buildup on East Antarctica that matches the oxygen isotope records of Shackleton and Kennett (1975) and Miller et al. (1991). They also suggest that glacial erosion removed much of the middle Miocene and younger section from the western Ross Sea shelf, making investigation of subsequent grounding events in this area difficult. Hayes et al. (1975) actually suggest that it was not until 4.5 Ma that the Ross Ice Shelf grew large enough to reach the northern limit of the shelf.

There is also terrestrial evidence of EAIS dynamics from the Antarctic continent that remains equivocal. Harwood and Webb (1998) claim that Pliocene diatoms found in the older Sirius Group of the Transantarctic Mountains were transported to the mountains by glacial ice after being eroded from marine strata in subglacial basins. This point of view suggests dynamic ice sheet behavior with advances and retreats through the Miocene and Pliocene. A contradictory view holds that the mountains received the diatoms via atmospheric wind transport (Stroeve et al., 1998). They claim that there is no need to invoke a dynamic view of ice sheet behavior; rather, the EAIS has likely been present and stable since the Miocene.

Investigation of the seismic record from the C-19 site will shed new light on the evolution of the EAIS. This closely spaced grid of seismic lines located in an up-dip location where older strata are closer to the seafloor provides an excellent opportunity to study a high-resolution data set in order to address some of the contradictions from previous studies. If sub-glacially deposited strata are present in the study area then chronostratigraphic correlation will yield an age for an ice shelf grounding event.

1.3 Project Overview

The high-resolution investigation of the early history of ice sheet fluctuations in the Ross Sea has been limited by the presence of the Ross Ice Shelf, which covers much of the strata that are of interest to seismic stratigraphers. In May of 2002, a large iceberg called C-19 calved from the Ross Ice Shelf (Arrigo and van Dijken, 2003). Exposed by this event was approximately 6400 km² of sea floor that has never been studied. The data sets of NBP 03-01 and NBP 03-06 (NBP = Nathaniel B Palmer) were acquired in this area and represent the

most up-dip section of the shelf ever imaged (Figure 1.2 and 1.3). Because of the up-dip location of this study area, it is now possible to look deeper into Antarctica's glacial history by looking at shallower occurrences of older strata with high-resolution techniques while avoiding the interference of the seafloor multiple. With the acquisition of this data set, it may now be possible to resolve the differences and shortcomings of the proxy data cited in the Previous Work section and finally offer direct evidence for the history of the EAIS grounding events in the Ross Sea.

The shortcomings of the proxy data for accurately dating these glaciation events leaves the timing of the first shelf-wide ice grounding event in the Ross Sea unanswered. An age for the onset of EAIS glaciation on the continental shelf may be determined by using high-resolution seismic stratigraphy to examine the glacial record in the Ross Sea. Understanding the mechanisms that cause ice sheet expansion and contraction is important because it has strong links to changes in eustasy, ocean circulation patterns and global climate system. Understanding the stratigraphy is also important because C-19 is a site survey for drilling programs. By examining the stratigraphic record of the Ross Sea continental shelf, a site that possibly experienced numerous grounding events due to its proximity to the ice sheet, we can evaluate the most direct evidence of change in volume of the EAIS through time.

1.4 Project Goals

1.4.1 Glacial History

To date, very few pre-Oligocene sediments have been sampled in the drill cores in the Ross Sea region, making sound interpretations difficult. Ultimately, answers to some of the

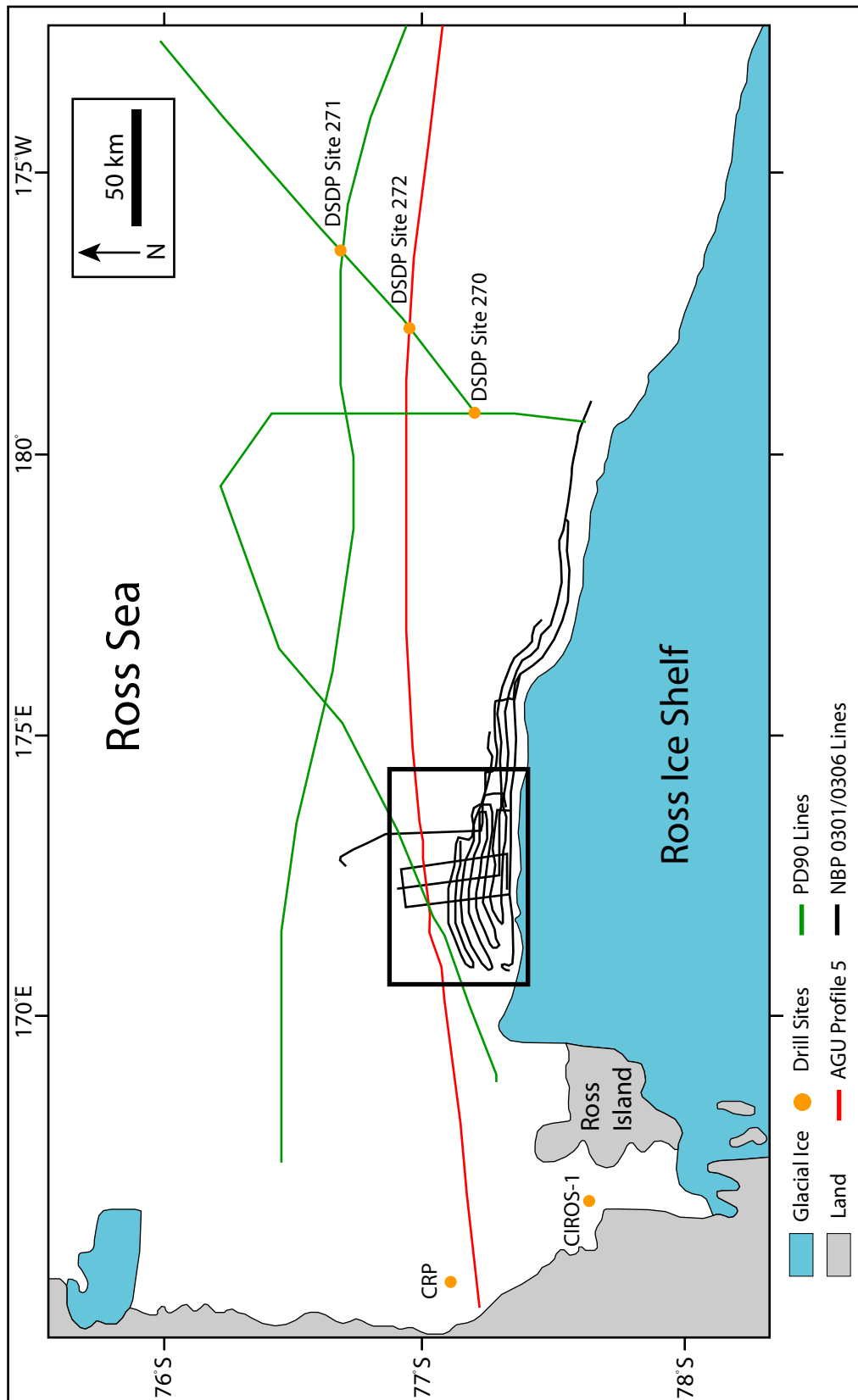


Figure 1.2 - Black box outlines C-19 study area. Colored lines show correlation paths from C-19 site to DSDP drill sites.

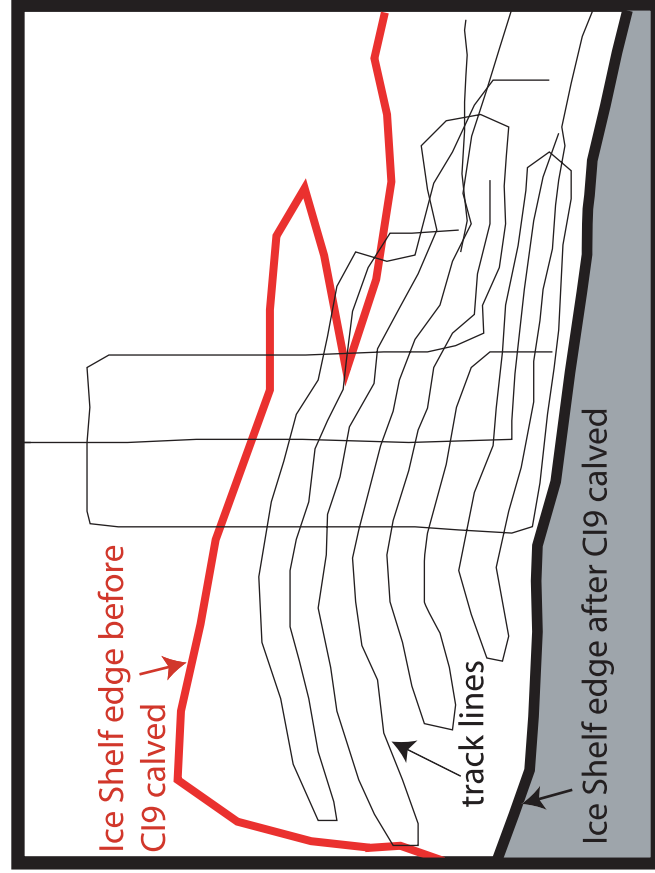


Figure 1.3 - Map of C-19 site showing track lines and position of ice shelf edge before and after calving of C-19 iceberg.

questions below will aid in future efforts to locate areas for drill sites and core samples as well as additional seismic profiles.

Goals of this project include: 1) Establish the onset of EAIS glaciation on the continental shelf in the Ross Sea by correlating stratigraphic surfaces from the C-19 site to Cape Roberts, CIROS and DSDP Leg-28 drill cores in order to establish a chronology for the C-19 stratigraphy. This provides an opportunity to determine whether the ice sheet grounding events in McMurdo Sound (CIROS-1 and Cape Roberts) are associated with local glacial activity or are part of continental-scale ice sheet advances. 2) Determine the history of the EAIS after initiation of glaciation on the shelf. That is, determine what events (glacial waxing and waning) took place and when they occurred and link these events to the climate, sea level and proxy records. 3) Characterize vertical facies association and lateral scales of heterogeneity.

The main objective of this project is to look for the first occurrences of glacial characteristics in the seismic records to better constrain timing for the onset of EAIS glaciation on the continental shelf and subsequent growth and decay cycles. The methods for identifying onset of large-scale glaciation include examining the reflection geometry, amplitudes, frequencies, lateral continuity and character of reflection terminations within the seismic stratigraphic units imaged with high-resolution single-channel seismic profiles for characteristics associated with sub-glacial deposition.

1.4.2 MCS Aliasing

The data sets of NBP-0301 and -0306 contain both single-channel seismic (SCS) and multi-channel seismic (MCS) profiles. Each type of seismic acquisition has advantages and

disadvantages. SCS data sets generally use a high frequency source signal to yield high-resolution seismic profiles (in the case of NBP-0301 and -0306 the source frequency is about 150 Hz and the resulting vertical resolution is approximately 3 meters). Comparatively, the advantages of MCS data lay in their ability to image deeper into to the sub-surface due to a lower frequency source and MCS signal processing which suppresses the seafloor multiple. Since the NBP data sets consist of both types of seismic data, a unique opportunity exists to compare known features from corresponding seismic lines in order to gain an understanding of how glaciogenic seismic facies translate from high-resolution SCS to lower resolution MCS.

CHAPTER 2

METHODS

2.1 Data Acquisition and Processing

The data sets of NBP 03-01 and NBP 03-06 were collected in January of 2003 and January of 2004, respectively, aboard the Research Vessel/Ice Breaker *Nathaniel B. Palmer*. NBP 03-06 acquired single-channel seismic (SCS) and multi-channel seismic (MCS) simultaneously. SCS acquisition used one 25/25 generator-injector (GI) gun and a 24 hydrophone streamer and MCS acquisition used six GI guns and a 48-channel streamer. The shot interval was 10 seconds with the SCS delayed by 7 seconds from the MCS. Ship speed was maintained at approximately 5 knots to ensure a constant shot spacing. NBP 03-01 acquired data with similar specifications. Multibeam, chirp sub-bottom and side-scan sonar data were also collected on these cruises.

Processing of both the SCS and MSC data was done using Seismic Processing Workshop (SPW) by Parallel Geoscience Corporation. SCS was processed with the intent of improving the signal/noise ratio and obtaining the highest possible resolution in the shallow portions of the seismic data. Processing included application of filters (bandpass was set to cut out frequencies lower than 50 Hz and higher than 600 Hz) to eliminate ambient noise and applying a spiking deconvolution to decrease the “ringy” character of the seismic lines and produce a stronger signal. The MCS was processed with the objectives of suppressing the

seafloor multiple and emphasizing the higher amplitude reflections at depth. MCS processing included filters set to eliminate frequencies lower than 10 Hz and higher 100 Hz.

2.2 Seismic Stratigraphic Analyses

Interpretations of the processed seismic data were made using The Kingdom Suite by Seismic Micro-Technology. Criteria outlined by Vail (1987) and Van Wagoner et al. (1988) were used as guidelines for interpretations. East-west oriented profiles along with north-south oriented profiles, forming a grid pattern on the Ross Sea continental shelf, were examined. The goals of the interpretation process include determining an age for the first appearance of glacial stratigraphy on the Ross Sea continental margin and characterizing the heterogeneity in the distribution of sediment facies and stratigraphic surfaces. The central method of interpretation is identifying reflection terminations to characterize stratigraphic units and variations in reflection attributes (amplitude, frequency, continuity and orientation) within the units.

Using sequence stratigraphic principles, four unconformity-bound sequences were identified, as well as seismic facies changes within the sequences. Reflection termination patterns, such as erosional truncation, were used to identify bounding surfaces of sequences (Figure 2.1). Seismic facies were classified based upon variation in amplitude, frequency, lateral continuity and reflection orientation (Figures 2.2, 2.3). Table 2.1 summarizes criteria for seismic facies classification.

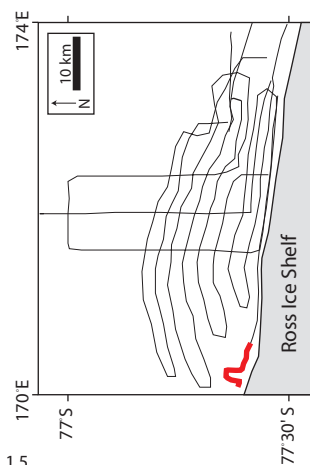
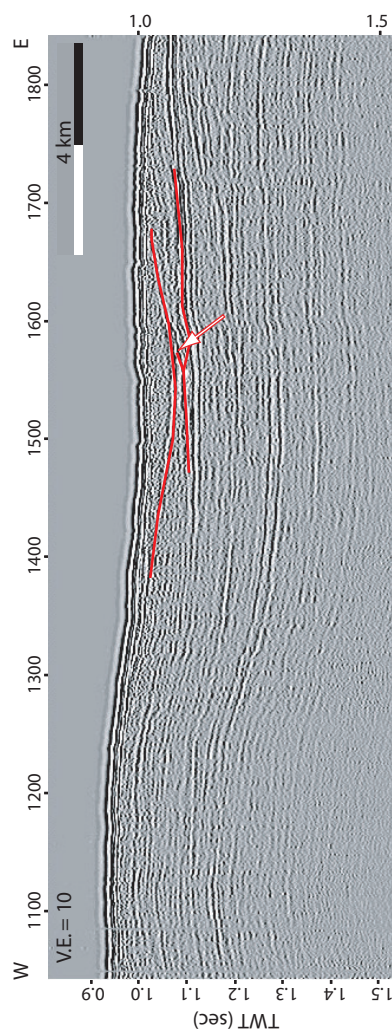
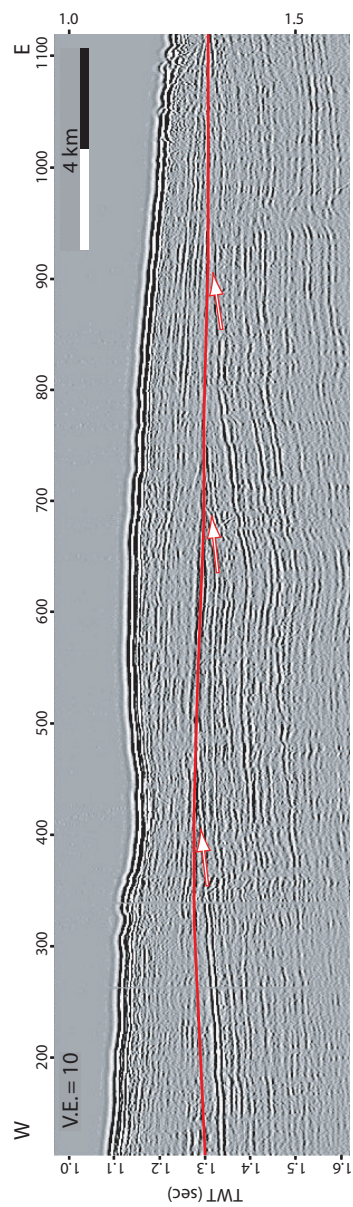


Figure 2.1 - Reflection termination patterns found in the study area, such as erosional truncation (top) and cross-cutting erosional truncation (bottom).

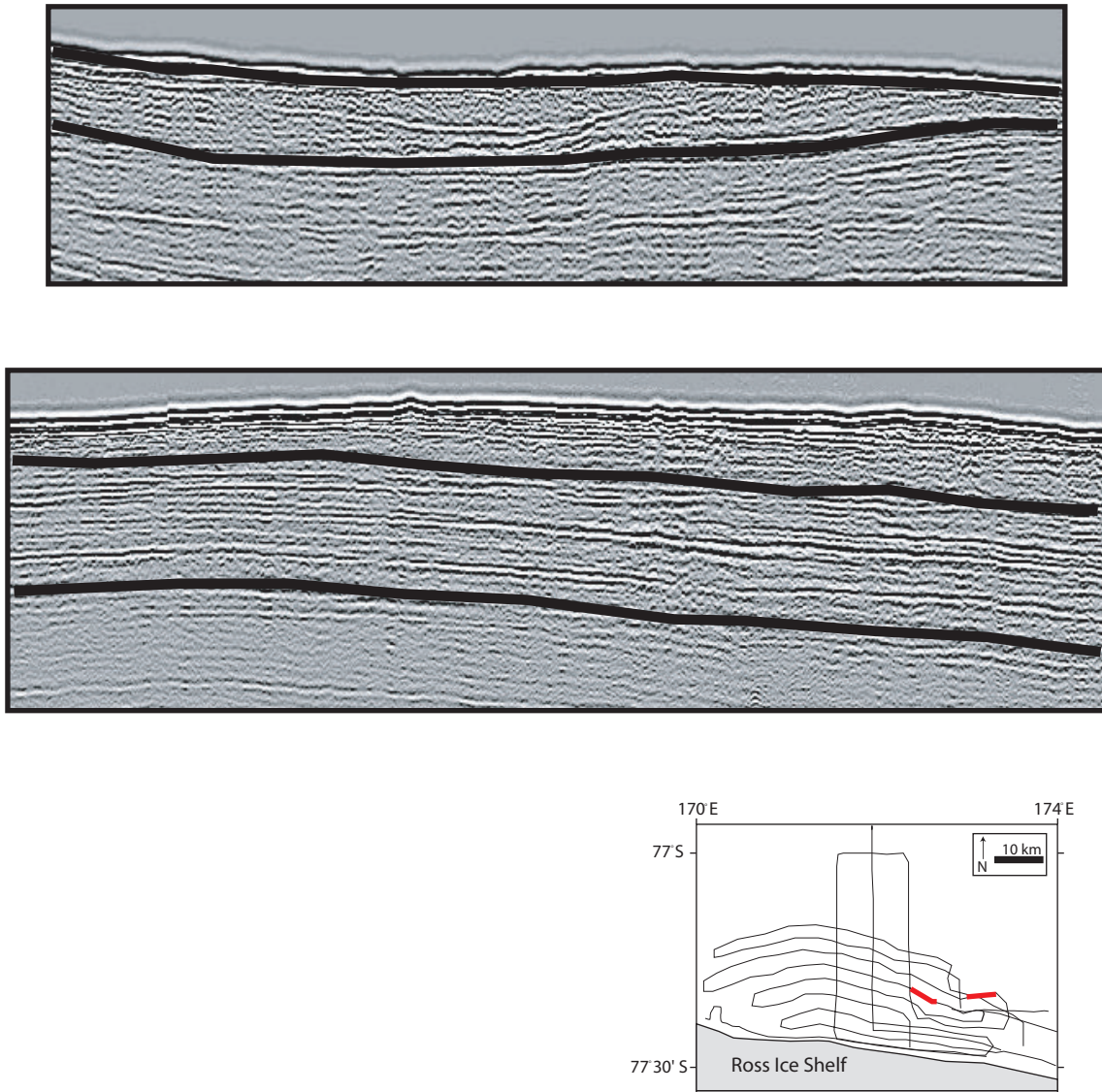


Figure 2.2 - Seismic facies standards outlined and labeled. Facies include variations in reflection frequency, amplitude, continuity and orientation. The upper seismic line displays laterally restricted cross-cutting reflections with high amplitude and medium frequency. The lower line displays laterally continuous, parallel reflections with high frequency and high amplitude.

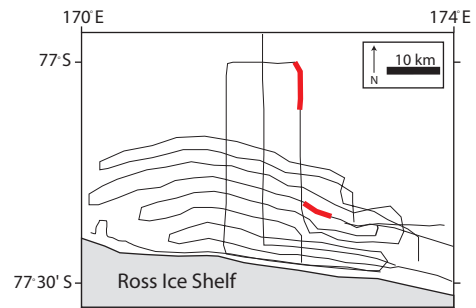
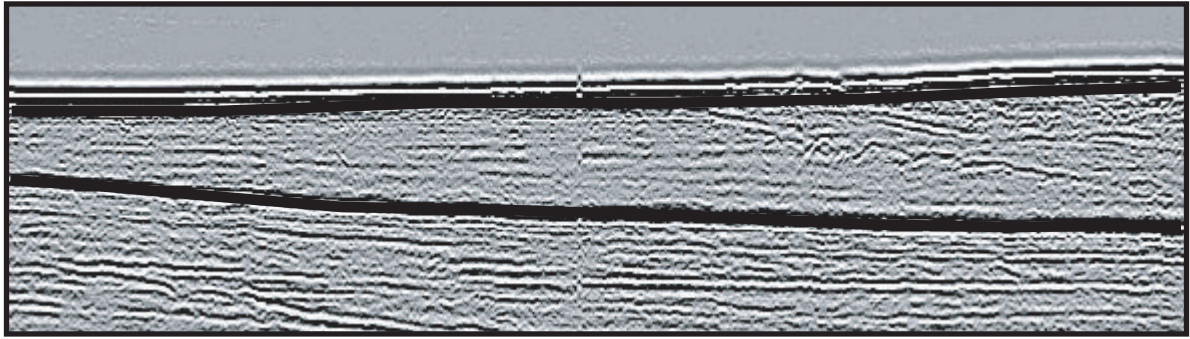


Figure 2.3 - Seismic facies standard outlined and labeled. Facies include variations in reflection frequency, amplitude, continuity and orientation. The upper seismic line displays a package with minimal internal reflections of a discontinuous nature with medium to high frequency and medium to high amplitude. The lower line displays laterally continuous, parallel reflections with low frequency and medium to high amplitude, with inter-layered reflection-free packages.




Lateral continuity	Low	< 1 km
	Medium	1 – 5 km
	High	> 5 km
Frequency	Low	< 3 reflections / 10 msec
	Medium	3 -6 reflections / 10 msec
	High	> 6 reflections / 10 msec
Amplitude	Low	
	Medium	
	High	

Table 2.1 – Criteria for classification of seismic facies.

2.3 Maps

Using the interpreted seismic data, structure maps (unit depth in time) and isochron maps (unit thickness) were generated and used to identify sites of erosion and deposition and the spatial distribution of units and facies. Isochron maps for the thicknesses of units and facies were made by determining the two-way-travel (TWT) time between two interpreted horizons to calculate a thickness in time. Depending on the sequence or facies mapped, the maximum projection distance was changed to limit the interpolation so as not to extend out beyond the range of confidence.

Facies distribution and environment interpretation maps were also made for each sequence. Facies maps were constructed by compiling all facies within a sequence on one

map using Adobe Illustrator. From these maps, environment interpretation maps were created based on the distribution of facies.

2.4 MCS Aliasing

Comparison of SCS and MCS profiles was done in Kingdom Suite. Reflection attributes such as amplitude, frequency, continuity and orientation were examined and findings summarized in table form (Table 3.1). Known glaciogenic features were examined using side-by-side comparison of MCS and SCS seismic profiles. Reflection attributes considered are summarized in table 2.1.

CHAPTER 3

RESULTS

3.1 Seismic Stratigraphy

The seismic stratigraphy of the C-19 site in the Ross Sea, Antarctica consists of seismic stratigraphic units with a range of facies attributes. All major units described in this section adhere to the “RSS-“ nomenclature (Ross Sea Sequence) put forth by Cooper et al. (1995). In this system, the units are dubbed RSS-2, RSS-3, RSS-4, with RSS-2 being the oldest, and their bounding unconformities (Ross Sea Unconformities) are labeled RSU-4, RSU-5, RSU-6, with RSU-6 being the oldest. Subunits and facies within the RSS units are described in terms of stratal geometry, such as variations in amplitude, frequency, continuity and termination patterns (see Methods), and relative positions, both vertical and horizontal.

RSS-2

Unit RSS-2 is present over the entire C-19 study site (Figure 3.1). This unit is bounded on top by a single high amplitude, laterally continuous reflection (RSU-5) that is conformable over most of the study site but has an angular relationship with the underlying strata in the eastern part of the grid (Figures 3.2, 3.3). The bottom of the unit is delineated by a high amplitude, laterally continuous but irregular reflection (basement) where it is not obscured by the multiple (Figure 3.1). This unit is subdivided into a lower and upper

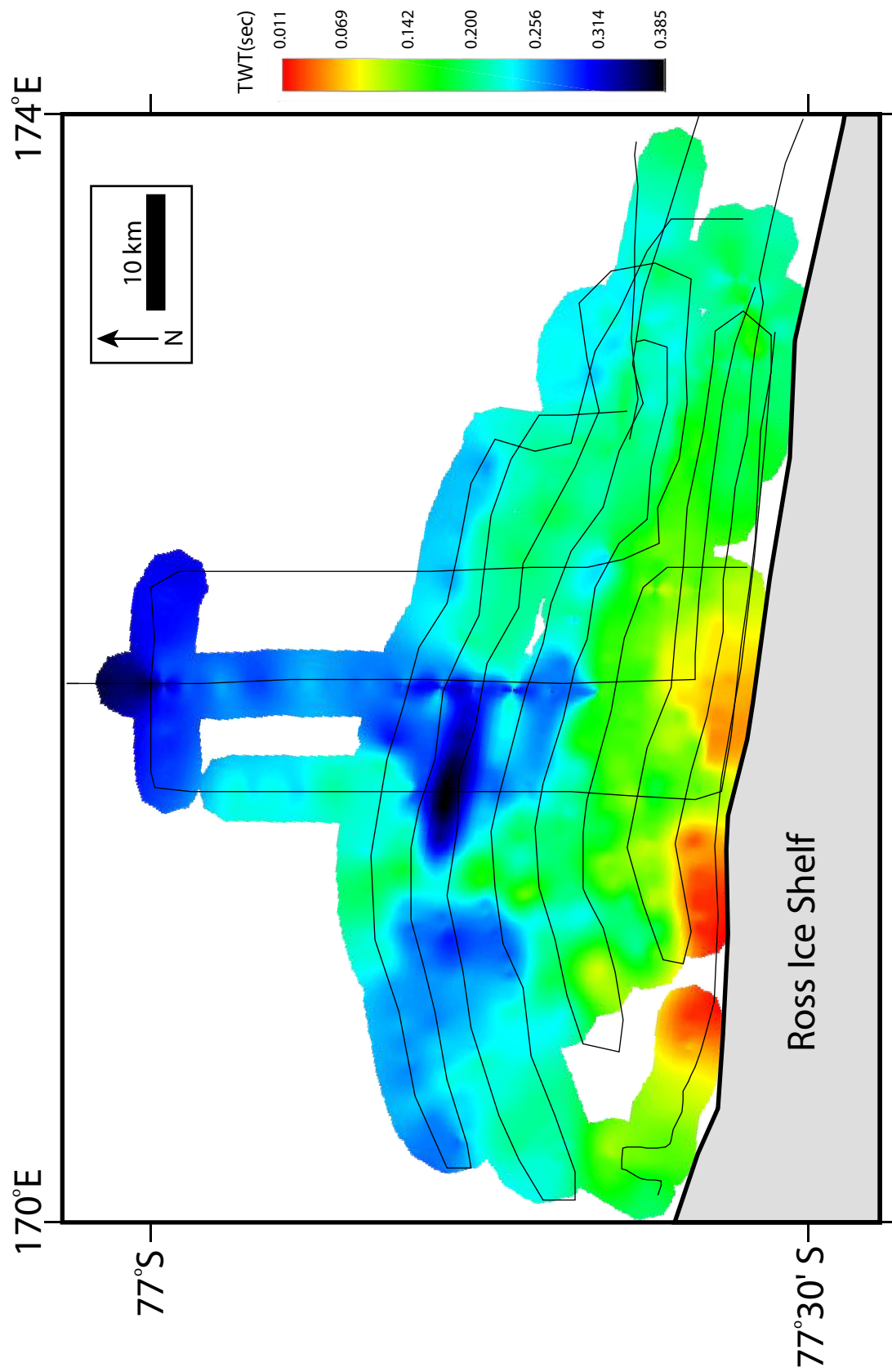


Figure 3.1 - Isochron map showing extent and thickness of the unit RSS-2

Line 8A

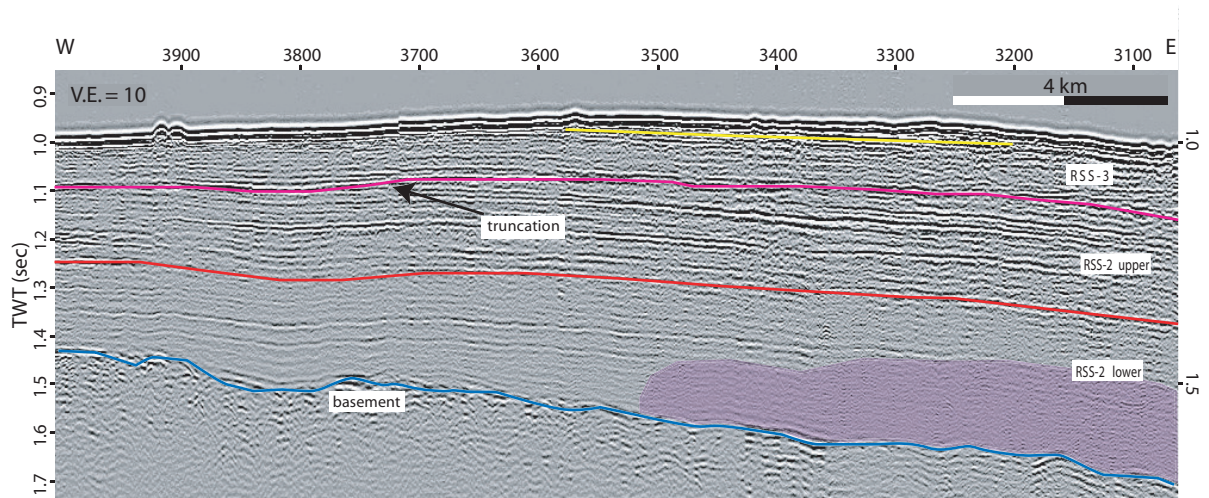
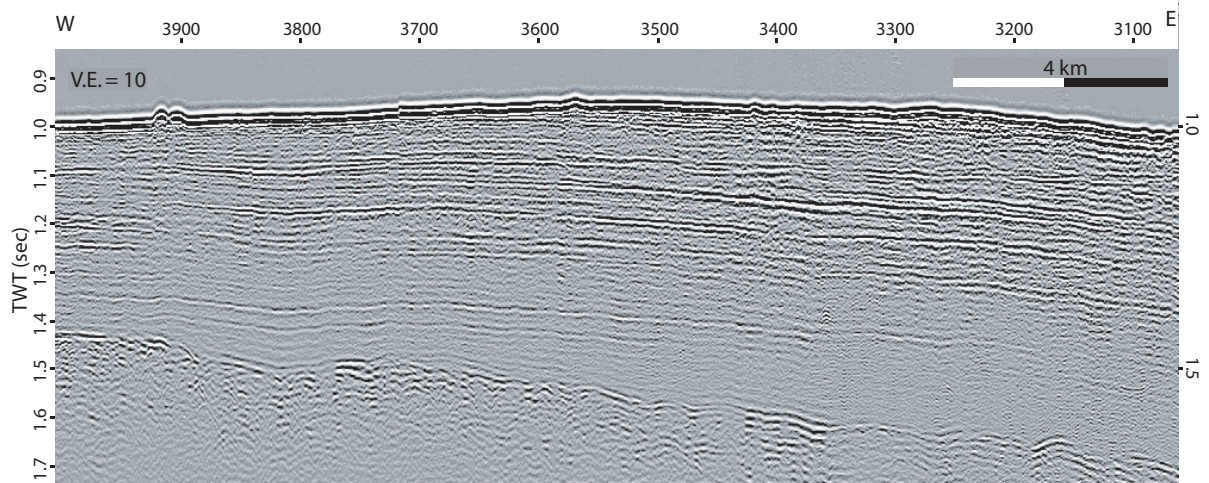
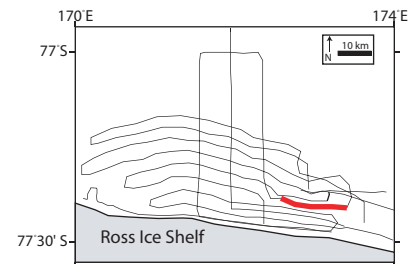


Figure 3.2 - Uninterpreted (top) and interpreted (bottom) seismic lines showing angular unconformity (pink line) RSU-5. Purple shaded area indicates decrease in amplitude of reflections. Location of line is shown of lower map.



Line 4D5

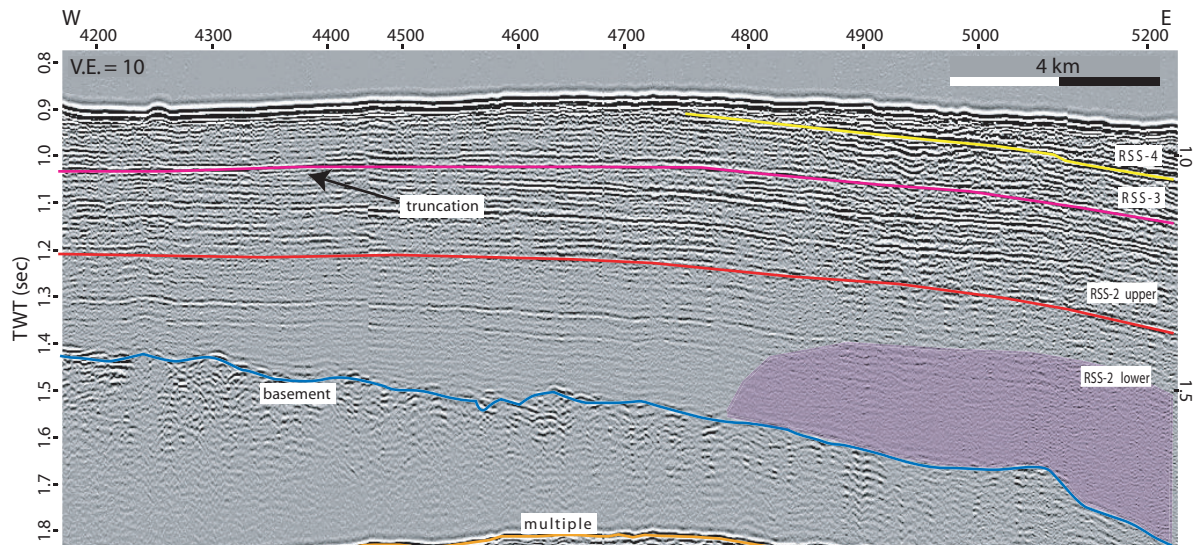
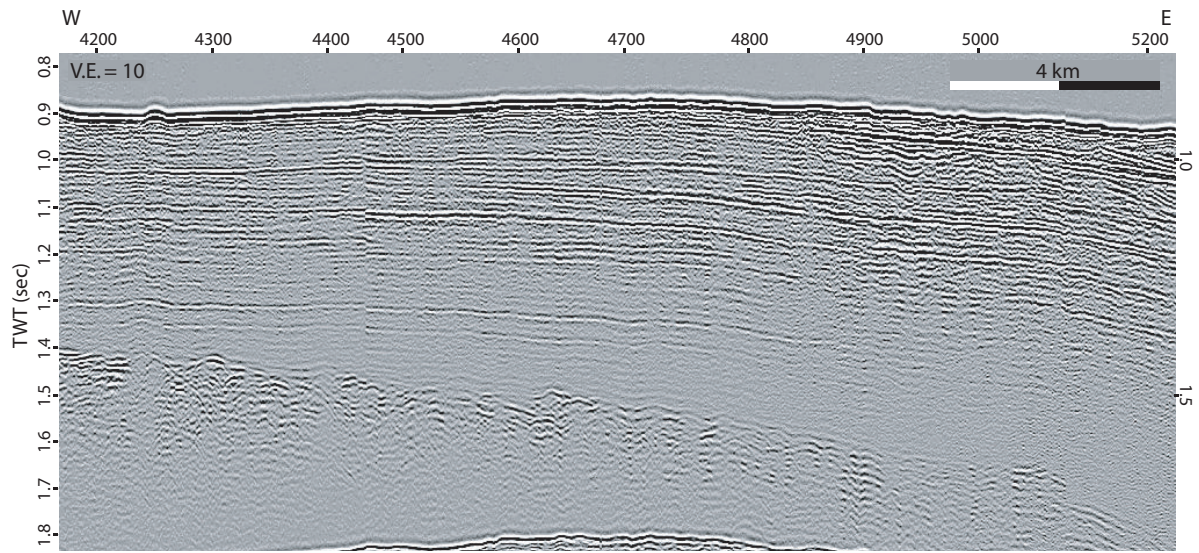
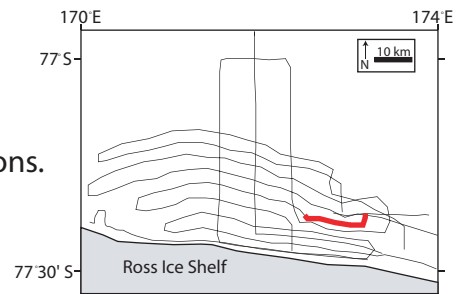


Figure 3.3 - Uninterpreted (top) and interpreted (bottom) seismic lines showing angular unconformity (pink line) RSU-5. Purple shaded area indicates decrease in amplitude of reflections. Location of line is shown of lower map.



section separated by a single, high-amplitude, laterally continuous reflection that is conformable over most of the site, but exhibits an angular relationship with the underlying strata in the southwestern portion of the study area (Figure 3.4).

Parallel, flat-lying, laterally continuous reflections ranging from medium to high amplitude and generally of low frequency dominate the lower section of this unit. The only change in seismic facies is an irregularly recurring decrease in amplitude throughout the entire thickness of the unit (Figures 3.2, 3.3). The strata above the unconformity in the upper section exhibit seismic characteristics similar to the lower section but in some areas have a higher frequency of reflections as well as higher amplitude (Figure 3.2).

RSS-3

RSS-3 is situated stratigraphically above RSS-2 and below RSS-4. This unit is present throughout most of the study area, except for the most up-dip third, where it is eroded completely by the modern seafloor unconformity bringing RSS-2 to the surface (Figure 3.5). The upper boundary is the same high amplitude reflection that marks the lower boundary for RSS-4 (RSU-4A). The lower boundary is the same high amplitude reflection that marks the top of RSS-2 (RSU-5).

Unit RSS-3 is divided into two main seismic facies; these facies are split along a north-south trend causing one facies to occupy the western part of the study site and the second facies to occupy the eastern part. The western facies consists mainly of reflection-free seismic facies with sporadic trough features (Figures 3.6, 3.7). The eastern facies consists primarily of trough cross-cutting features with internal packages represented by wavy to chaotic and reflection-free characteristics (Figures 3.8, 3.9).

Line 1A

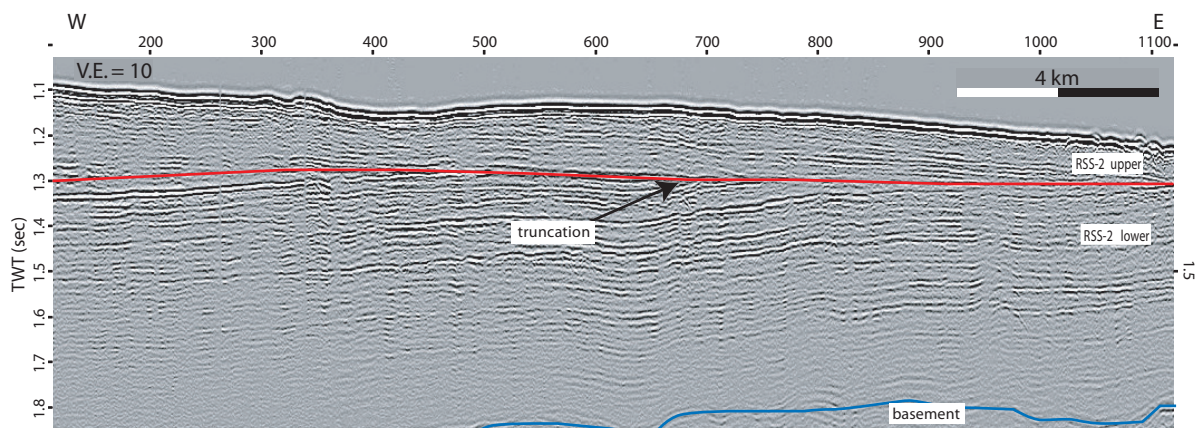
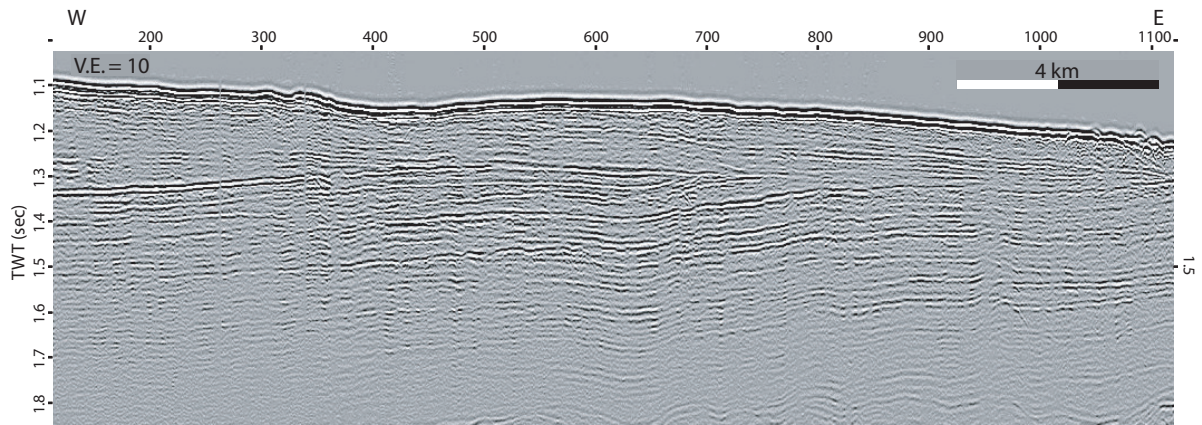
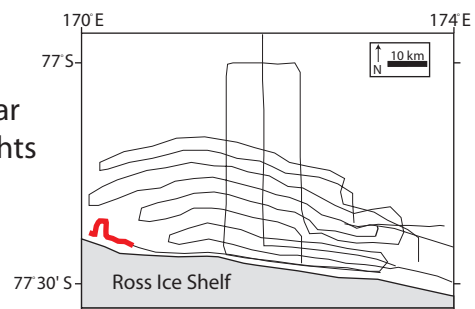


Figure 3.4 - Uninterpreted (top) and interpreted (bottom) seismic line showing angular unconformity within RSS-2. Red line highlights unconformity. Location of line is indicated on lower map.



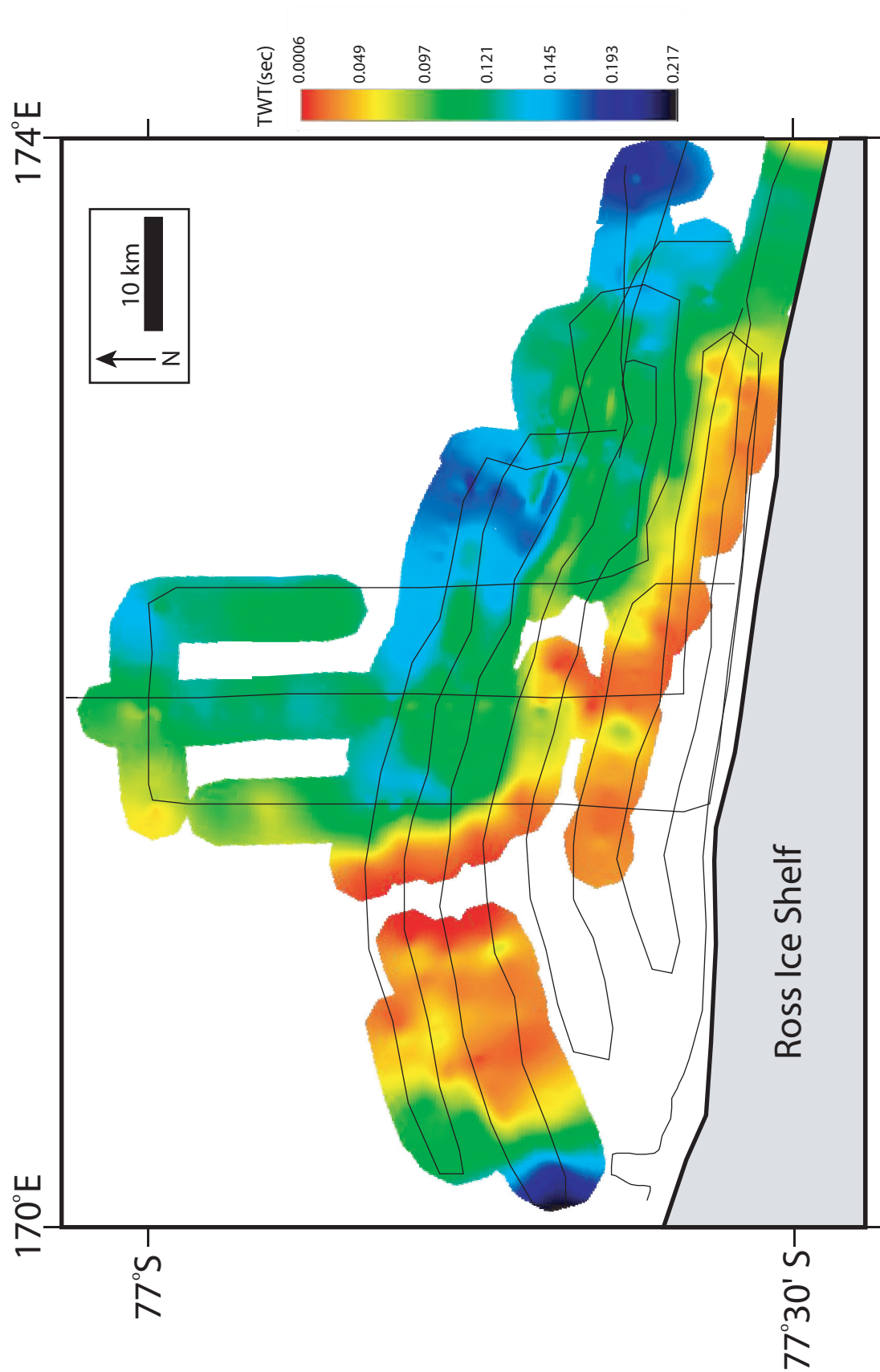


Figure 3.5 - Isochron map showing extent and thickness of the unit RSS-3

Line 6A1

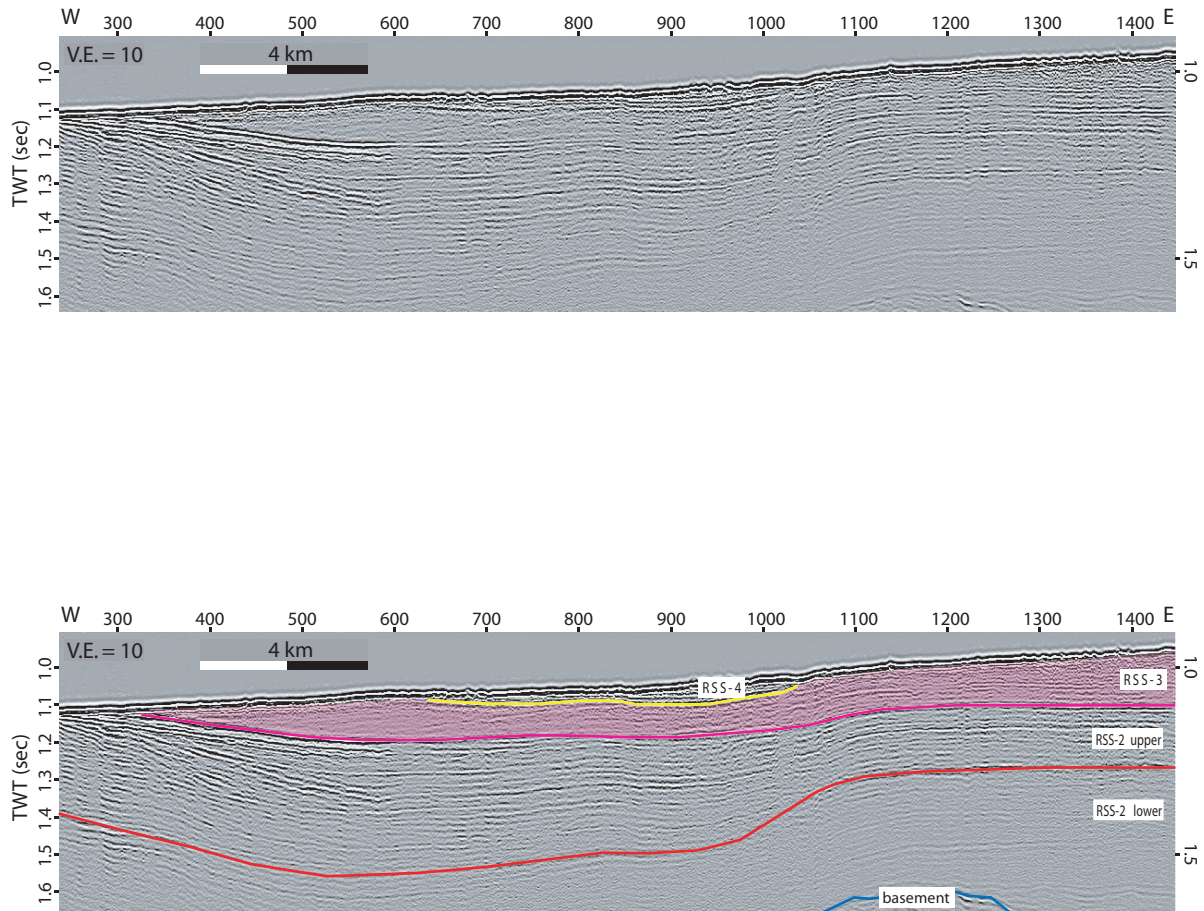
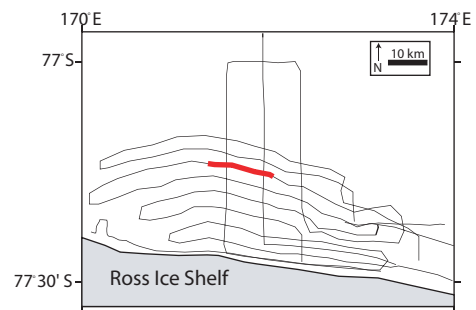


Figure 3.6 - Uninterpreted (top) and interpreted (bottom) seismic line showing minimal internal reflections of unit RSS-3 (shaded pink). Location of line is indicated on lower map.



Line 11A

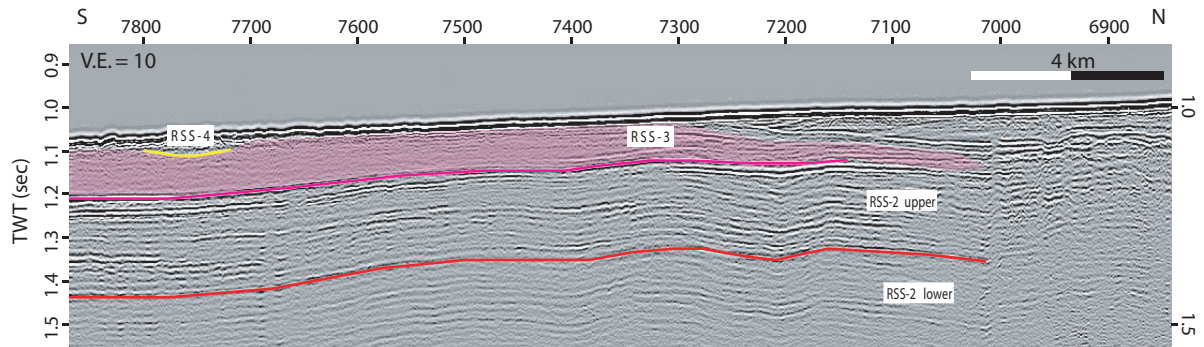
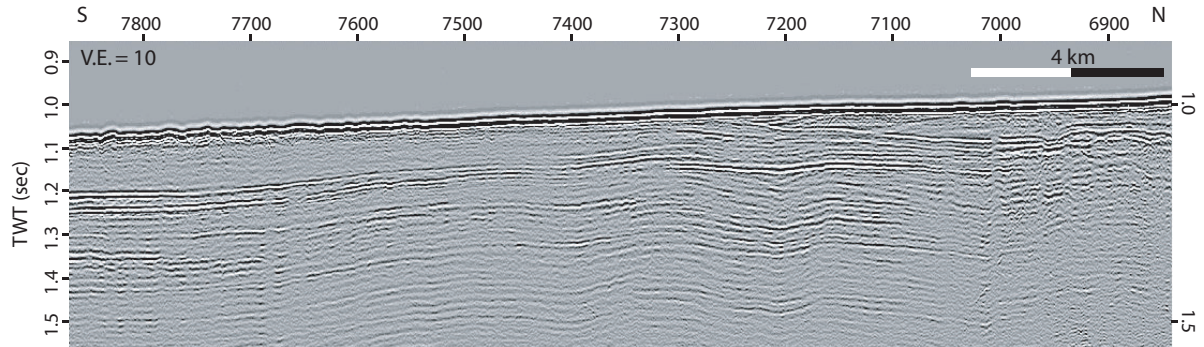
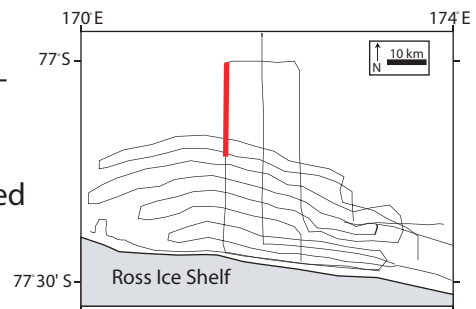


Figure 3.7 - Uninterpreted (top) and interpreted (bottom) seismic line showing minimal internal reflections of unit RSS-3 (shaded pink). Location of line is indicated on lower map.



Line 0306-2A

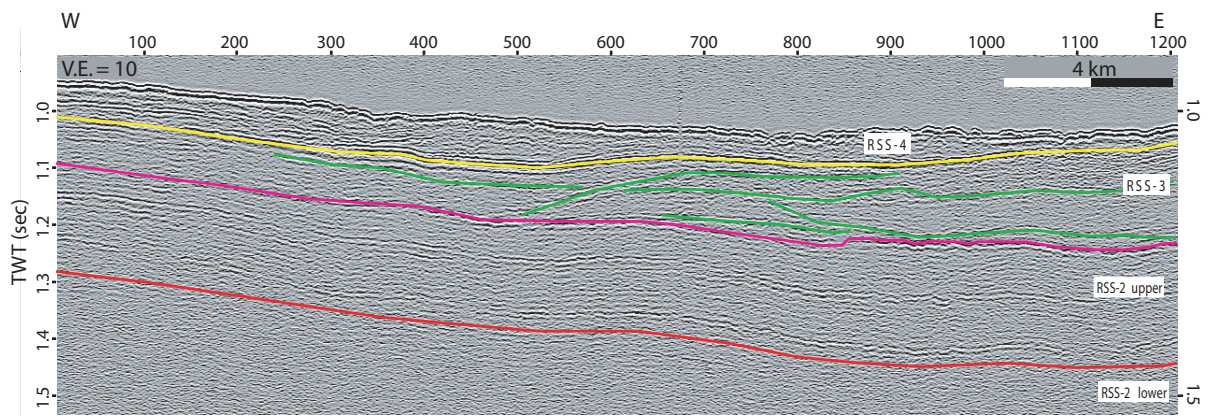
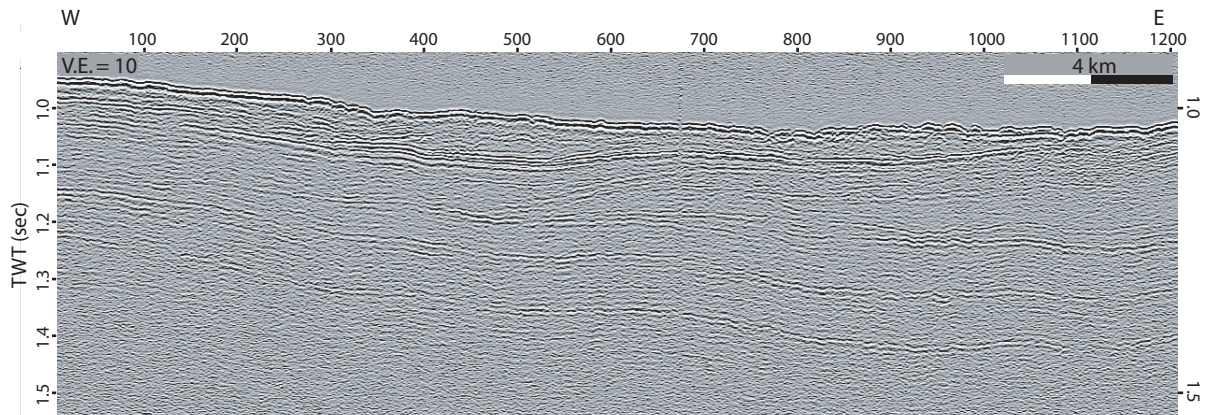
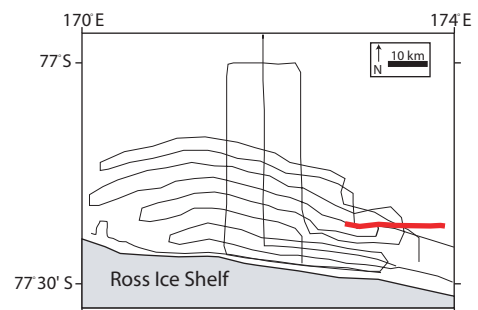


Figure 3.8 - Uninterpreted (top) and interpreted (bottom) seismic line showing cross-cutting reflections of unit RSS-3 (green lines). Location of line is indicated on lower map.



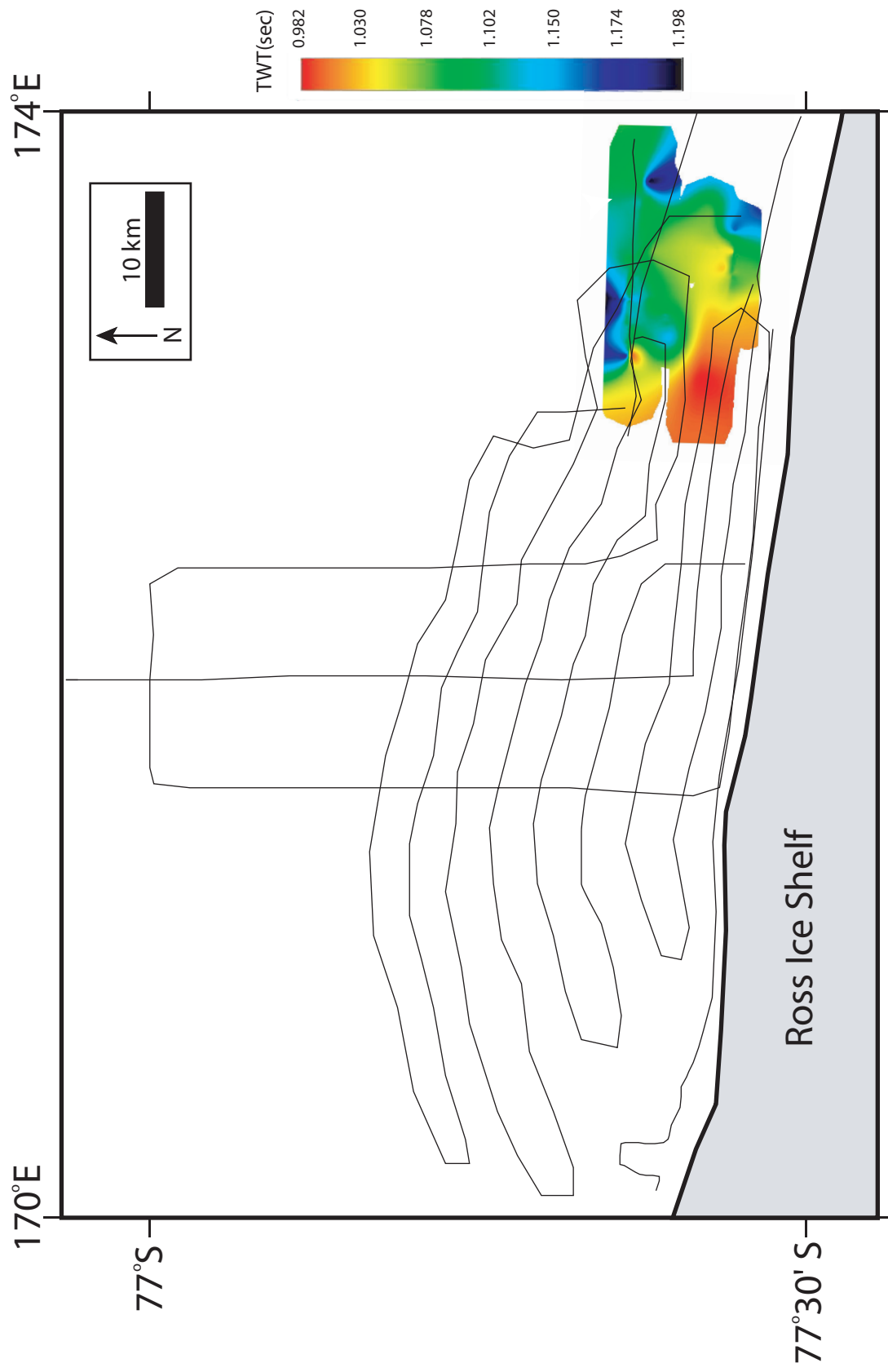


Figure 3.9 - Isochron map showing extent and thickness of the eastern facies of unit RSS-3

RSS-4

Unit RSS-4 is the shallowest unit in the study area, with the seafloor being the upper boundary. There are areas where it was removed by erosion, bringing unit RSS-3 to the surface. The lower boundary is a single high amplitude reflection with moderate relief over the study area and periodic truncation by the seafloor (RSU-4A). The distribution of RSS-4 is mainly restricted to the down-dip half of the study site (Figures 3.10). It appears to have been completely removed from the up-dip half of the study site by the seafloor unconformity.

This unit exhibits seismic facies varying from nearly reflection-free (Figure 3.11) to more chaotic and slightly wavy characteristics, all with little to no internal structure, with sporadic trough shaped reflections, the density of which become markedly increased in the eastern part of the study area (Figures 3.12, 3.13, 3.14).

3.2 MCS Aliasing

The data sets of NBP-0301 and -0306 contain both single-channel seismic (SCS) and multi-channel seismic (MCS) profiles. Each type of seismic acquisition has advantages and disadvantages. SCS data sets generally use a high frequency source signal to yield high-resolution seismic profiles (in the case of NBP-0301 and -0306 the source frequency is about 150 Hz and the resulting vertical resolution is approximately 3 meters). Comparatively, the advantages of MCS data lay in their ability to image deeper into the sub-surface due to a lower frequency source and MCS signal processing which suppresses the seafloor multiple. Since the NBP data sets utilize both types of seismic data, a unique opportunity exists to compare known features from corresponding seismic lines in order to

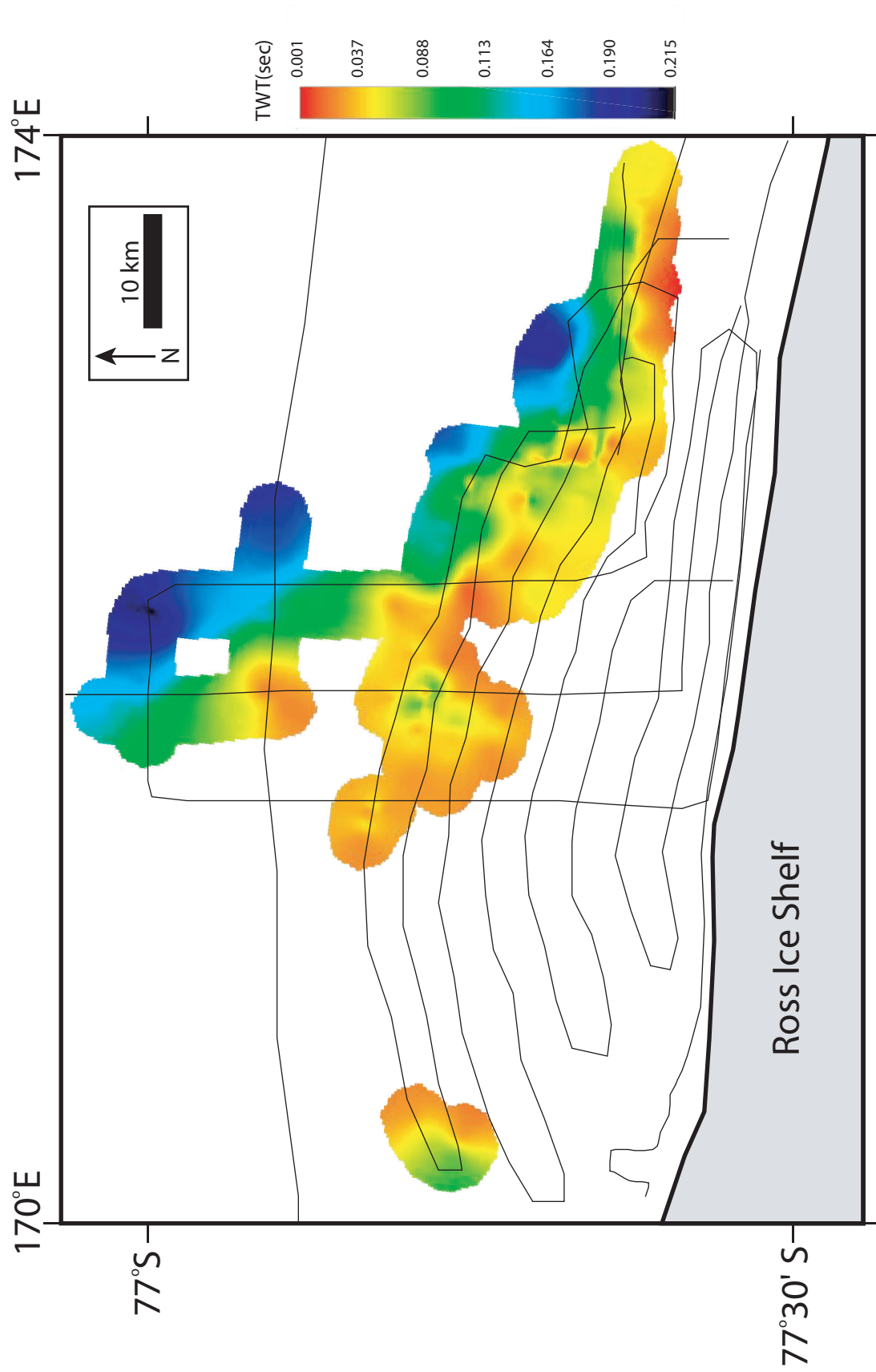


Figure 3.10 - Isochron map showing distribution and thickness of unit RSS-4

Line 9A

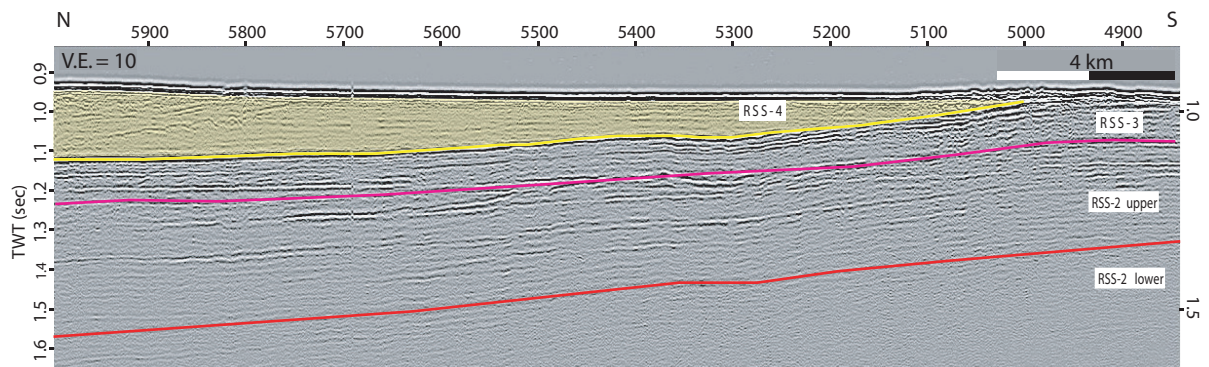
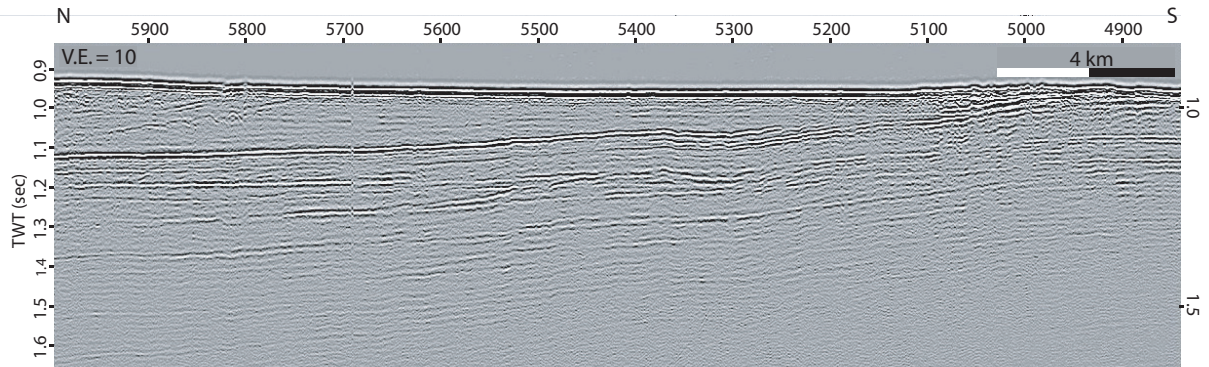
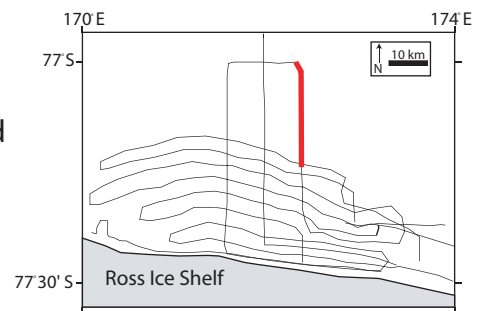


Figure 3.11 - Uninterpreted (top) and interpreted (bottom) seismic line showing minimal internal reflections of unit RSS-4 (shaded yellow). Location of line is indicated on lower map.



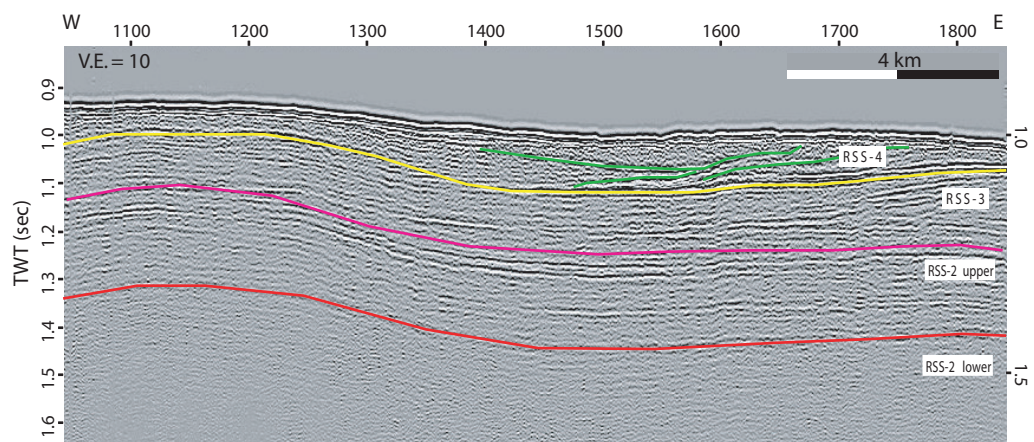
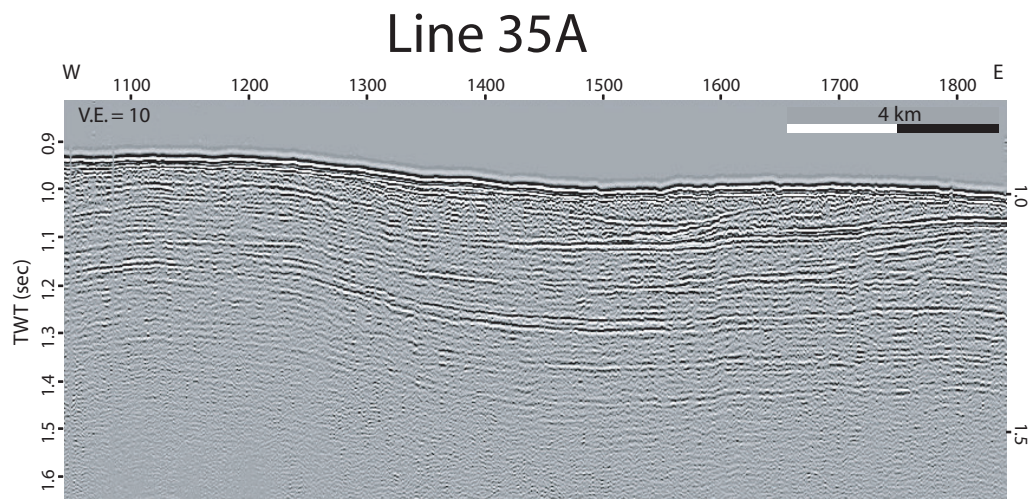
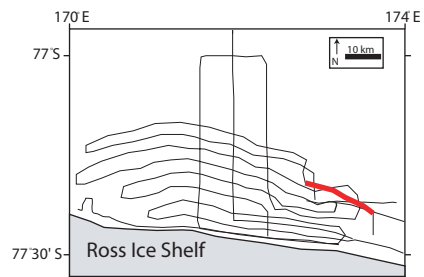


Figure 3.12 - Uninterpreted (top) and interpreted (bottom) seismic line showing cross-cutting reflections of unit RSS-4 (green lines). Location of line is indicated on lower map.



Line 7A

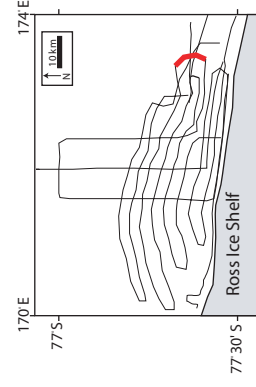
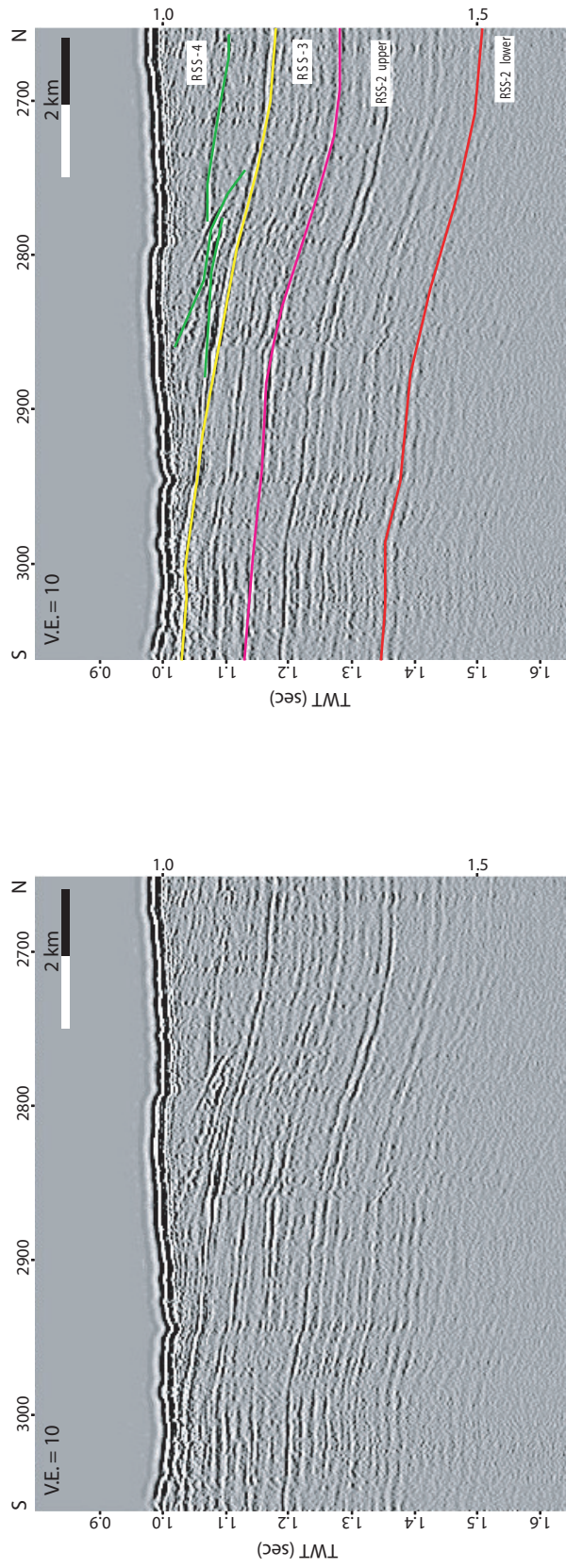


Figure 3.13 - Uninterpreted (top) and interpreted (bottom) seismic line showing cross-cutting reflections of unit RSS-4 (green lines). Location of line is indicated on lower map.

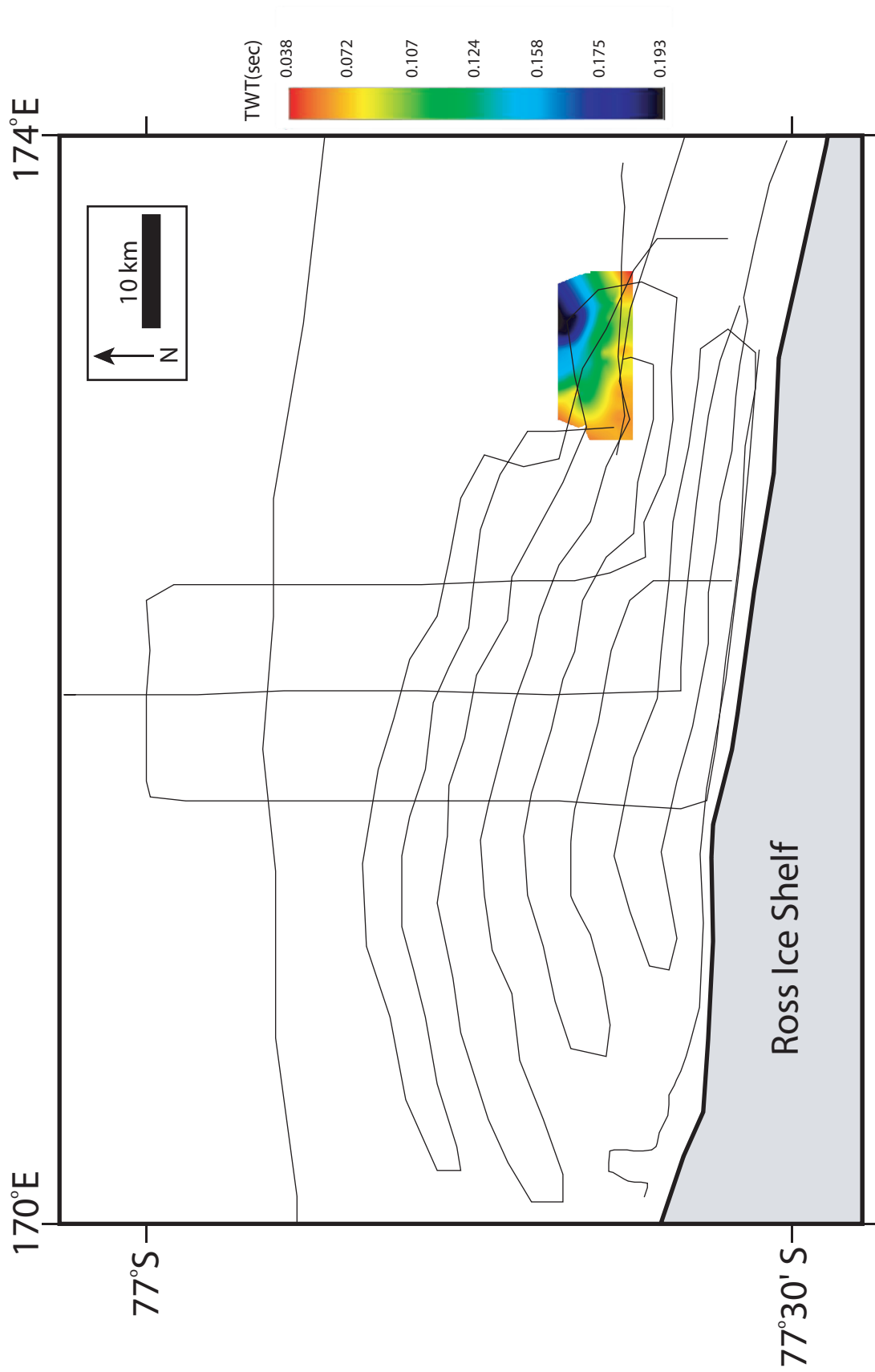


Figure 3.14 - Isochron map showing extent and thickness of the eastern facies in unit RSS-4

gain an understanding of how glaciogenic seismic facies translate from high-resolution SCS to lower resolution MCS.

Table 3.1 summarizes the differences and similarities of SCS and MCS. Described here are some of the key findings. In the upper two units found in site C-19, RSS-3 and RSS-4, glacial stratigraphy dominates. One of the most noticeable features in these units is the presence of reflection-free or near reflection-free packages. In SCS profiles these packages encompass completely reflection-free and mostly reflection-free packages with minimal internal reflections. However, in MCS profiles, these two distinct seismic facies appear as the single seismic facies of reflection-free strata (Figure 3.15).

Another key difference between SCS and MCS is a decrease in vertical resolution, which results in seismic facies that have a high frequency of reflections in SCS and a lower frequency in MCS. This is more noticeable in shallower strata (above dashed line, Figure 3.16). This reduction of frequency manifests itself in two ways. The first is a decrease in frequency of individual reflections (individual reflection look much more “crisp” in SCS). As seen in figure 3.15 (box), individual reflections become wider in MCS. In this particular example the indicated reflections spans 20 ms (TWT) in the SCS profile and 35 ms (TWT) in the MCS profile. This reduction in individual reflection frequency leads to fewer reflections per unit time (TWT). This can result in multiple layers of strata (as seen in SCS) being imaged as a single layer in MCS.

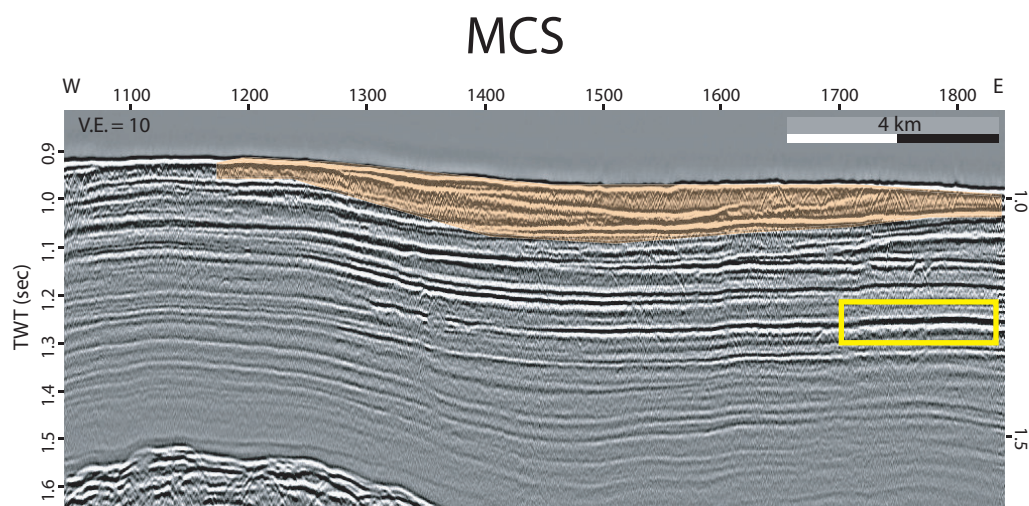
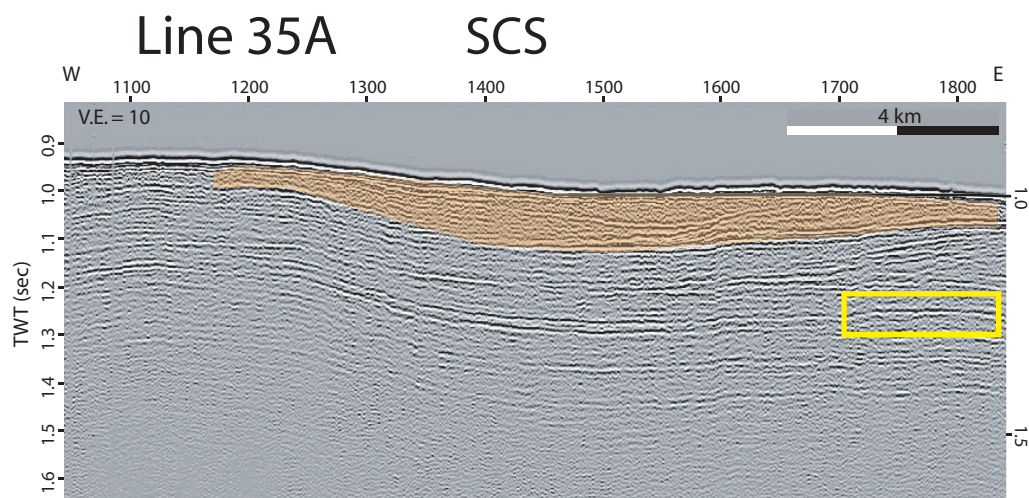
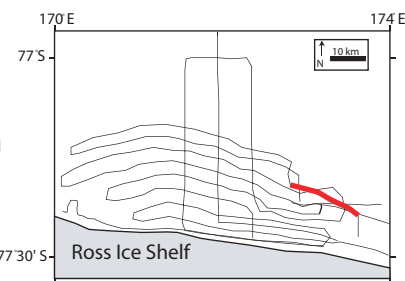


Figure 3.15 - SCS (top) and MCS (bottom) seismic lines. Orange shaded area highlights area where differences in reflection-free strata can be observed. Box indicates a single reflection that have a high frequency (small width) in SCS and lower frequency (wider) in MCS. Location of line is indicated on lower map.



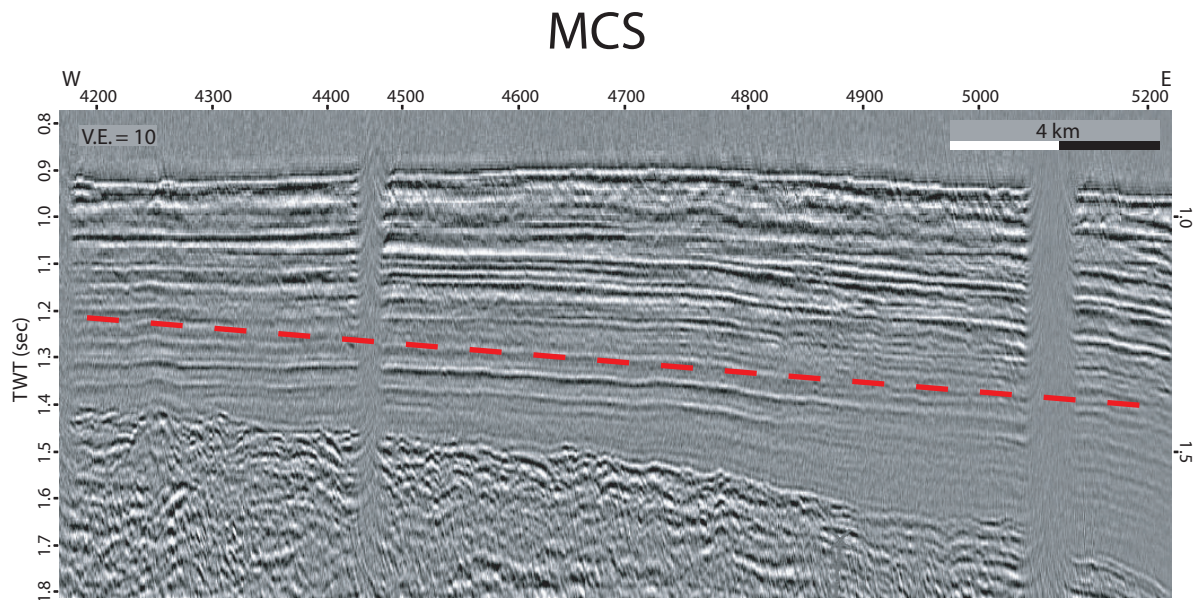
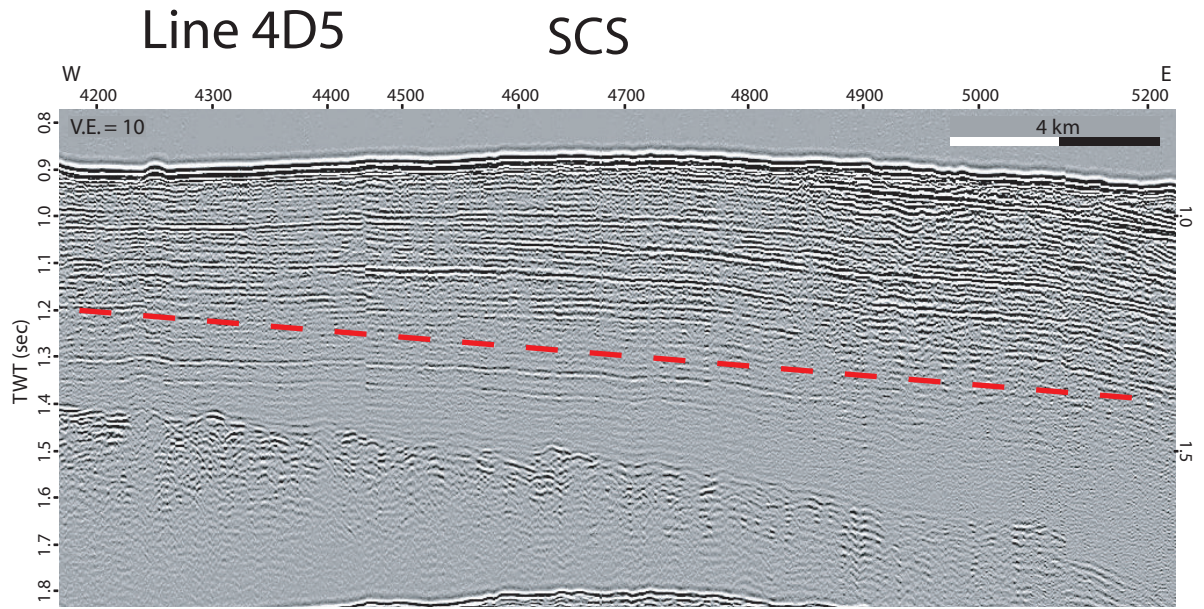
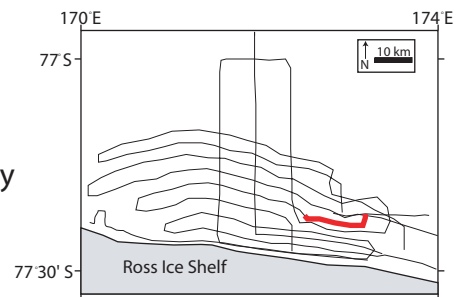


Figure 3.16 - SCS (top) and MCS (bottom) seismic lines. Above dashed line the number of reflections per unit time (TWT) is lower in MCS than SCS; below dashed line the frequency of reflections remains the same. Location of line is indicated on lower map.



Unit	SCS facies	MCS facies
<i>RSS-2</i>	Low to medium amplitude, low frequency reflections interlayered with reflection-free packages	Reduction in frequency of individual reflections; number of reflections per unit time remains unchanged
	High amplitude, high frequency reflections	High amplitude, medium frequency reflections
<i>RSS-3</i>	Reflection-free	Reflection-free
	Mostly reflection-free with minimal internal reflection	Reflection-free
	Cross-cutting troughs with reflection-free packages	Individual reflections that make up troughs have a lower frequency
<i>RSS-4</i>	Reflection-free	Reflection-free
	Mostly reflection-free with minimal internal reflection	Reflection-free
	Cross-cutting troughs with reflection-free packages	Individual reflections that make up troughs have a lower frequency

Table 3.1 – Table summarizing comparisons between SCS and MCS seismic facies.

CHAPTER 4

DISCUSSION

4.1 Chronostratigraphy

Correlation of the units present in the C-19 study area with regional drill sites provides chronostratigraphic control. C-19 sequences adhere to the nomenclature Cooper et al. (1995) put forth for sediments in the Ross Sea. The units are named “RSS-“ sequences, with units RSS-2, RSS-3 and RSS-4 (RSS-4 = youngest) present in the study area. These units are dated by the DSDP Leg 28 drill sites (Hayes and Frakes, 1975), with the oldest recovered rocks being from the upper RSS-2 unit and dating to the late Oligocene (circa 25 Ma) based on foraminifera from site 270 (Leckie and Webb, 1986). The correlation path from the C-19 site, composed of seismic lines from the NBP 0301 and NBP 0306 data sets, goes through the PD90 (Polar Duke) data set as well as AGU Profile 5 (Figure 1.2).

4.2 Sequence Interpretations

RSS-2

The oldest strata in the C-19 study area lie within unit RSS-2. Correlation of these strata with the DSDP drill site constrains the age of the oldest sediments drilled to the late Oligocene (25 Ma). The seismic signature of the lower portion of the RSS-2 unit, which lies below the reach of the drill core and is therefore of unknown age, exhibits parallel, flat-lying,

laterally continuous reflections with varying amplitudes (medium and high) and relatively low frequency reflections interlayered with uniformly thick reflection-free packages (Figure 3.2, 3.3). Two opposing scenarios may have produced the seismic facies described above.

In the first scenario the low to medium amplitude reflections are interpreted as erosional unconformities produced when the EAIS advanced out onto the Ross Sea continental shelf. The interlayered reflection-free packages are interpreted as ice-proximal facies deposited as the ice sheet advanced toward the site. In this situation, the EAIS would have to contain an ice volume during the Oligocene at least as large as the modern ice sheets in order to surpass modern day ice limits. Zachos et al. (2001) suggest that the EAIS was a temperate ice sheet after the initial build-up of ice during the early Oligocene and remained so through the late Oligocene. In the aforementioned scenario, a temperate ice sheet advancing out onto the continental shelf leaving behind erosional unconformities and ice-proximal sediments would have likely also left behind other signatures in the seismic record. In this seismic interval there is a lack of substantial topographic relief, which is typically associated with glacial unconformities, indicating that grounded ice did not produce the low to medium amplitude reflections. Temperate ice sheets are generally accompanied by meltwater runoff. Meltwater features often appear in the seismic record as fluvial channel systems (Donda et al., 2007). The seismic facies of RSS-2 in the C-19 study area lack any features consistent with meltwater, also indicating that ice was not grounded during this interval. Another feature used to investigate the nature of the ice at this time is glacial lineations. Lineations are linear gouges left behind on the seafloor after the retreat of grounded ice. Again, the lower RSS-2 unit in the study area lacks lineations, supporting the ice-free interpretation. Finally, as seen in figures 3.2 and 3.3, there are areas where the low

to medium amplitude reflections undergo a loss of amplitude and seem to fade away. All other glacial unconformities in the study area maintain their high amplitudes through the entire C-19 site. All of these lines of evidence point to an alternative hypothesis for the creation of interlayered low to medium amplitude reflections and reflection-free packages.

The competing hypothesis, which seems more likely due to the lack of definitive evidence of a grounded ice sheet, is that the low to medium amplitude reflections were deposited as condensed sections, or maximum flooding surfaces, when the ice sheet retreated far from the study site and the reflection-free packages were deposited as ice-distal to ice-proximal facies as the ice sheet moved toward the study site but did not reach it (Figure 4.1, 4.2). The seismic stratigraphic analysis of these strata indicate that this advance and retreat cycle occurred at least ten times. This scenario precludes the presence of grounded ice in the C-19 study site on the Ross Sea continental shelf during the time that the lower section of unit RSS-2 was deposited, possibly the early to middle Oligocene.

The lower section of RSS-2 is separated from the upper portion by a single high amplitude reflection that is interpreted as a regional unconformity. This reflection is noticeable as an angular unconformity in the southwestern part of the C-19 site in seismic line 1A (Figure 3.4) but is conformable over the rest of the study area. The strata of RSS-2 that lie above this unconformity exhibit similar seismic characteristics to the lower section except for having higher frequency of reflections and higher amplitude in places (Figure 3.2). It is possible that the strata in the lower section of RSS-2 and the upper section were deposited in the same sedimentary environment. If this is the case, then the observed differences in the frequency and amplitude of the reflections may be explained by attenuation of the source signal. It is also possible that the higher frequency and amplitudes in the upper

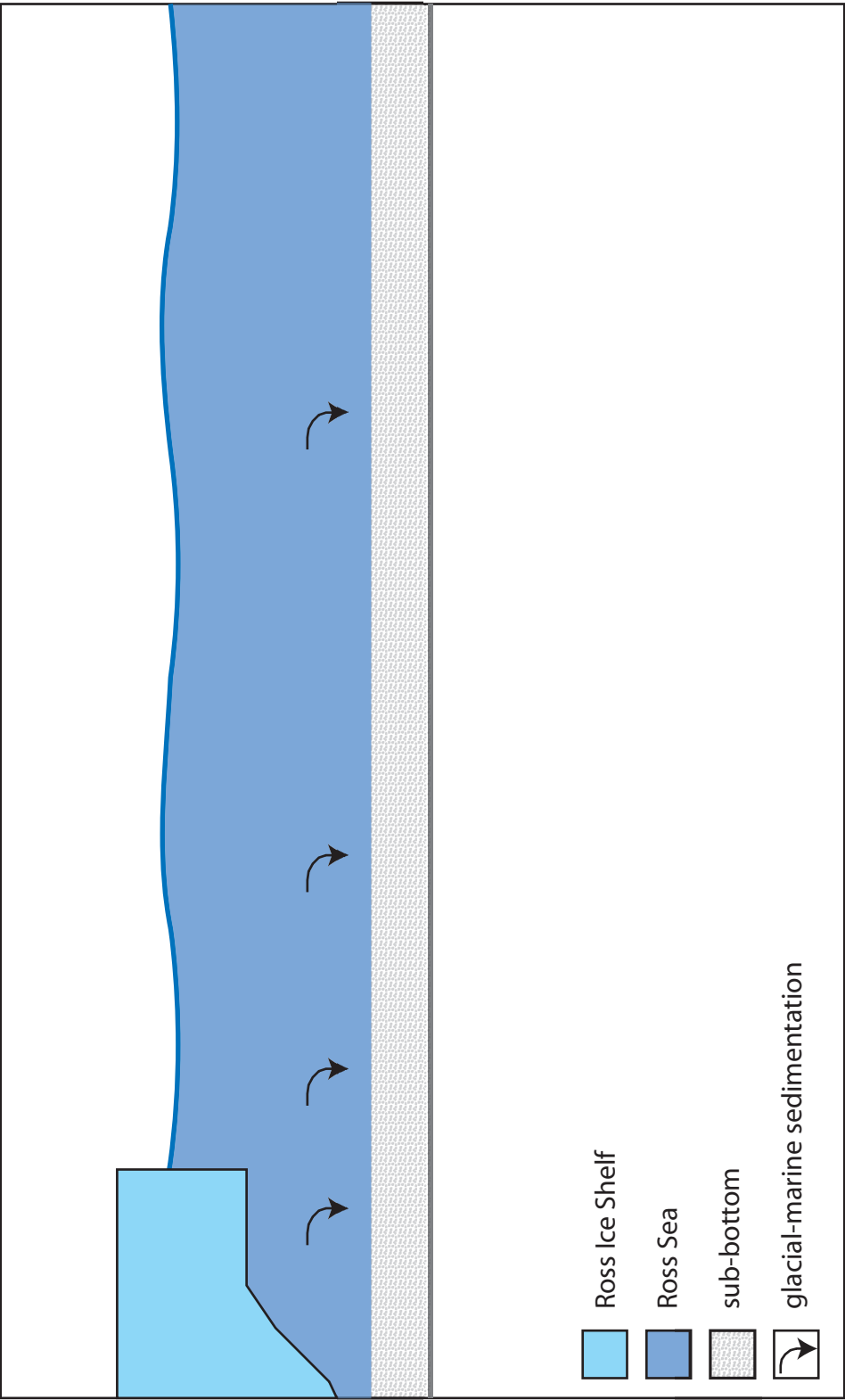


Figure 4.1 - Illustration showing deposition of ice-distal to ice-proximal sediments producing reflection-free strata during period when ice is approaching the site.

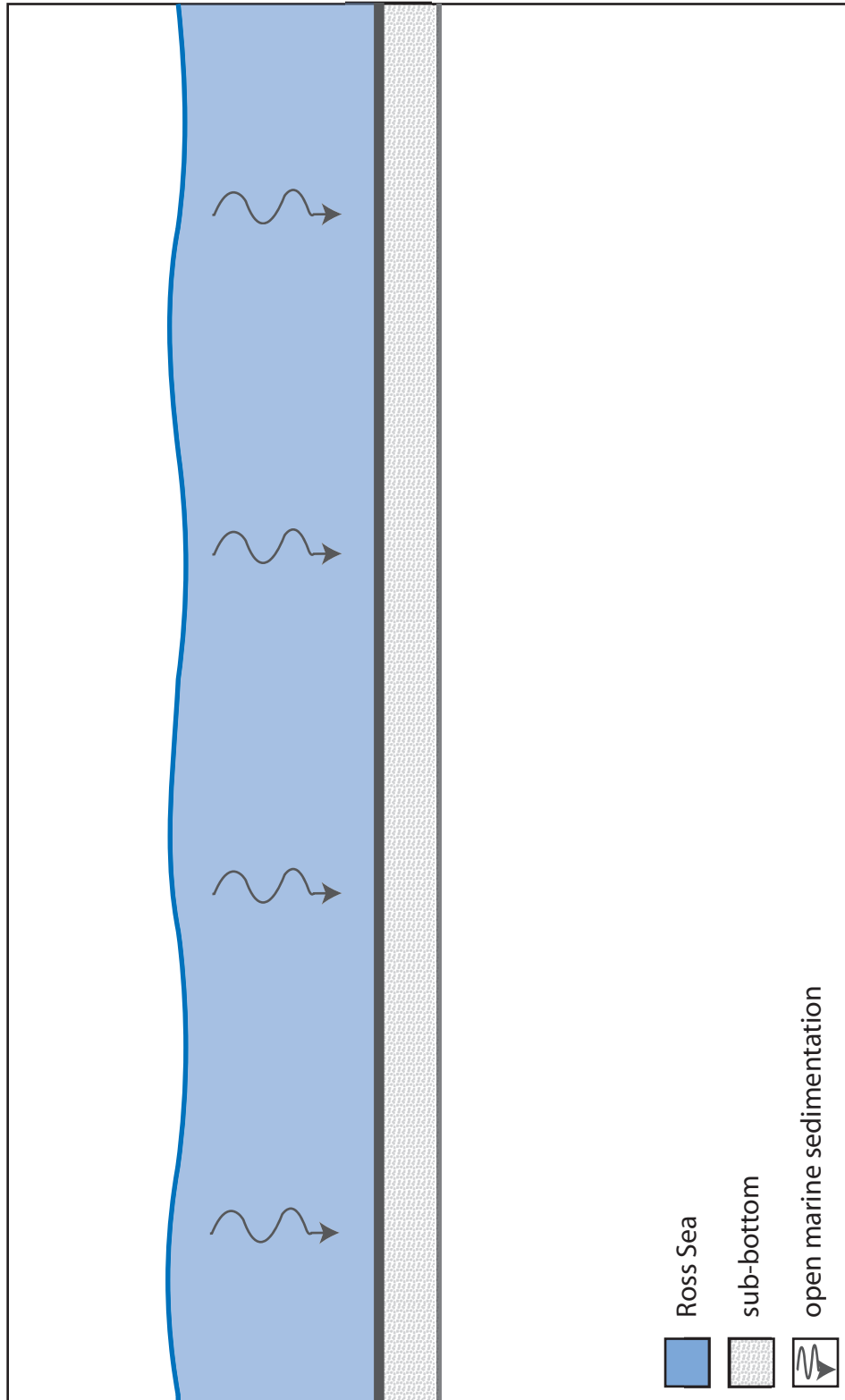


Figure 4.2 - Illustration showing normal marine sedimentation during an ice-free period producing high amplitude condensed section (bold gray line) on top of reflection-free strata.

sections are the result of differential sedimentation processes. If the ice sheet progressively approaches closer to the study site during the time of deposition of the upper section, then an increase in grain size of the glacial-marine sediments could produce a higher impedance contrast giving the strata higher amplitude reflections. In both scenarios, the strata of the upper section of unit RSS-2 are interpreted to be of non-glacial and glacial-marine origin and not sub-glacial. This means that the unconformity that separates the lower section from the upper section is likely the result of a sea-level drop without concomitant glacial advance onto the Ross Sea continental shelf. The strata of the upper section of unit RSS-2 date to the late Oligocene, so these interpretations offer evidence against ice grounding on the shelf in the C-19 region at any time during the Oligocene.

The upper section of unit RSS-2 in the southwestern part of the C-19 site exhibits seismic strata somewhat different from the rest of study area. Here the nature of the reflections changes from parallel, laterally continuous with high frequency and high amplitude to discontinuous reflections with near reflection-free areas (Figure 3.4). The nature of this seismic facies change is difficult to interpret. While it is clearly not of the same origin as the rest of the upper RSS-2 unit, the seismic characteristics are not definitive enough to yield a glacial interpretation.

RSS-3

The boundary between the oldest unit, RSS-2, and the younger unit, which sits stratigraphically above it, RSS-3, is a regional unconformity, named RSU-5, that is mutually parallel with the overlying and underlying strata over most of the study site but is evident as an angular unconformity in the eastern section of the site. This unconformity dates to the

early Miocene and is interpreted as a glacial erosion surface and represents the first regional ice sheet grounding event seen in the C-19 study area (Figure 4.3). The strata above this unconformity lie within unit RSS-3 and clearly show glacial features (Figure 3.12).

Two separate but similar seismic facies dominate unit RSS-3. The western portion is mostly reflection-free while cross cutting unconformities abound in the eastern section (Figure 4.4). The strata that are either reflection-free or have few and weak internal reflections indicate that the sediment is overcompacted or was massively deposited, as in a sub-glacial or ice-proximal environment (Anderson, 1999). The strata dominated by cross-cutting unconformities exhibit abrupt lateral truncation of sediment packages which indicates erosion in a sub-glacial environment (Bart and Anderson, 1997). This type of seismic facies is often described as cut and fill, suggesting the power of grounded ice sheets to dynamically erode and deposit sediment, specifically by the actions of fast-moving ice streams within the ice sheet.

RSS-4

The boundary between the youngest and stratigraphically shallowest unit, RSS-4, and the underlying RSS-3 unit is the regional unconformity called RSU-4A. This unconformity is visible as a site wide high amplitude reflection (Figure 3.11). This unconformity is interpreted as a glacial erosion surface and, based on correlation to the DSDP drill sites, dates to the early to middle Miocene. The strata within the overlying unit, RSS-4, are remarkably similar to the strata of RSS-3. There is a similar division of seismic facies from the western portion of the study site to the eastern part. As seen in RSS-3, largely reflection-free strata are found in the west and cross-cutting unconformities in the east (Figure 4.5).

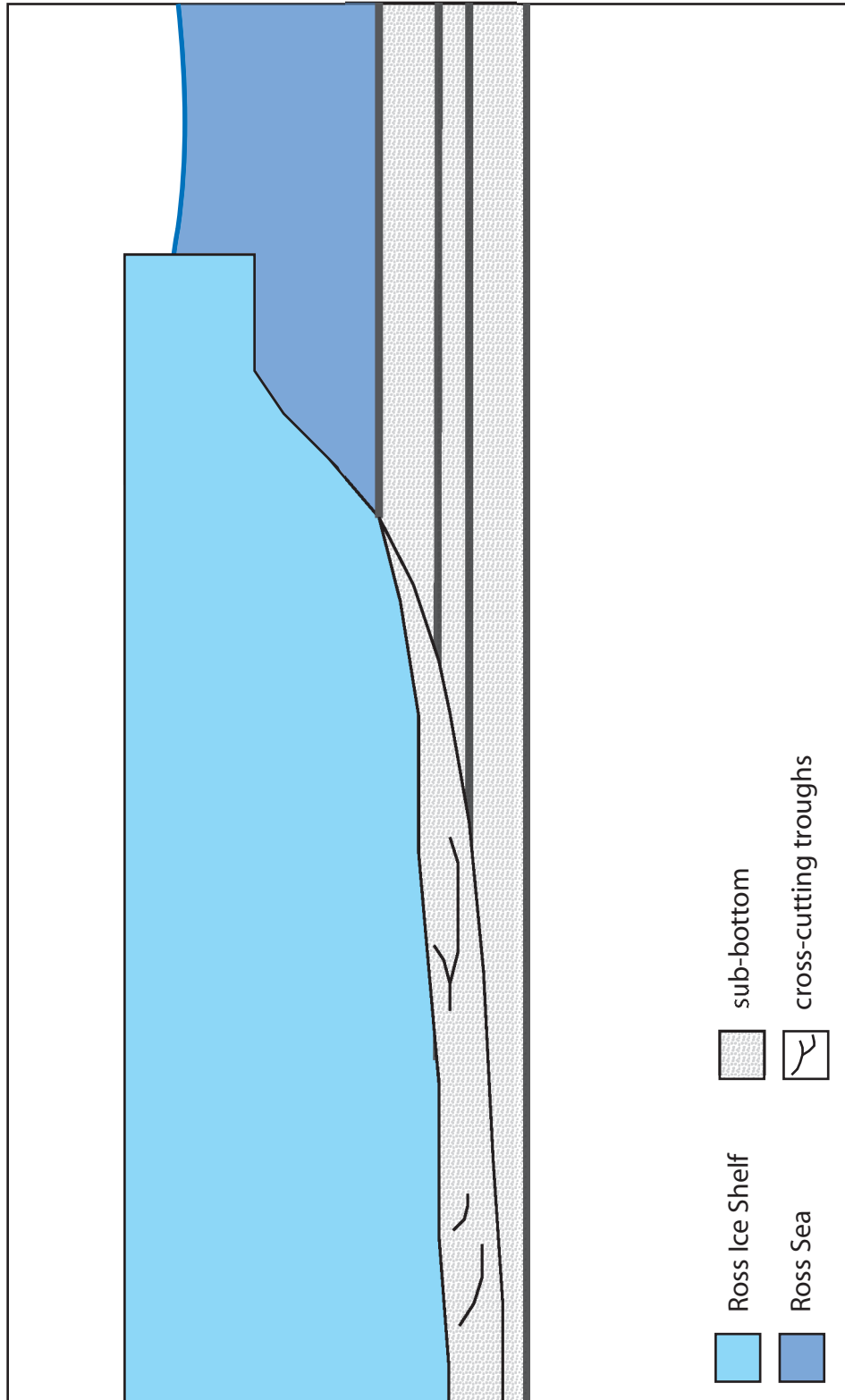


Figure 4.3 - Illustration showing sub-glacial deposition subsequent to deposition of multiple cycles of ice-proximal and ice-free sediments. Sub-glacial strata are largely reflection-free with scattered erosional troughs.

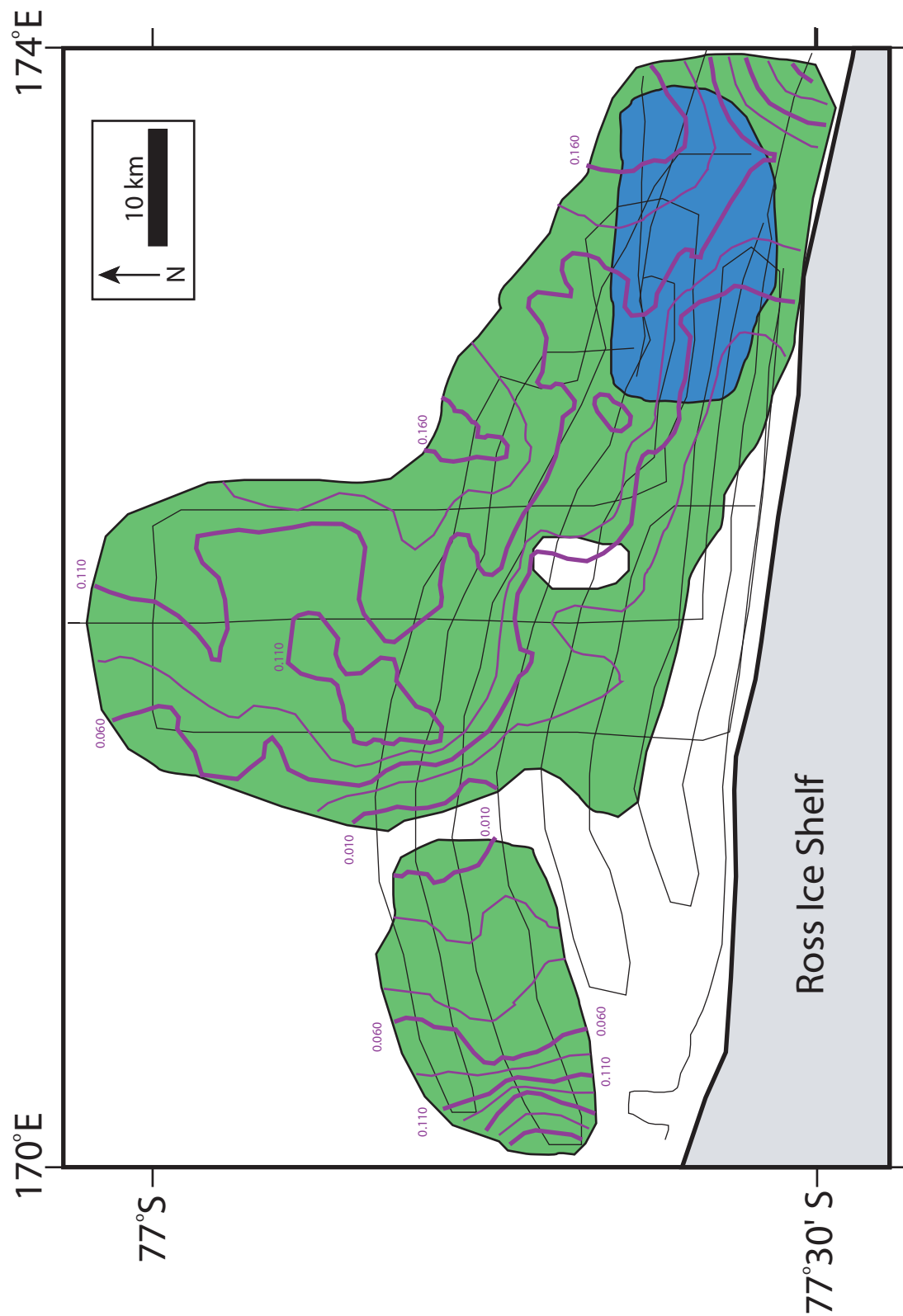


Figure 4.4 - Facies map of unit RSS-3 showing location of mostly reflection free strata (green) and cross-cutting strata (blue).

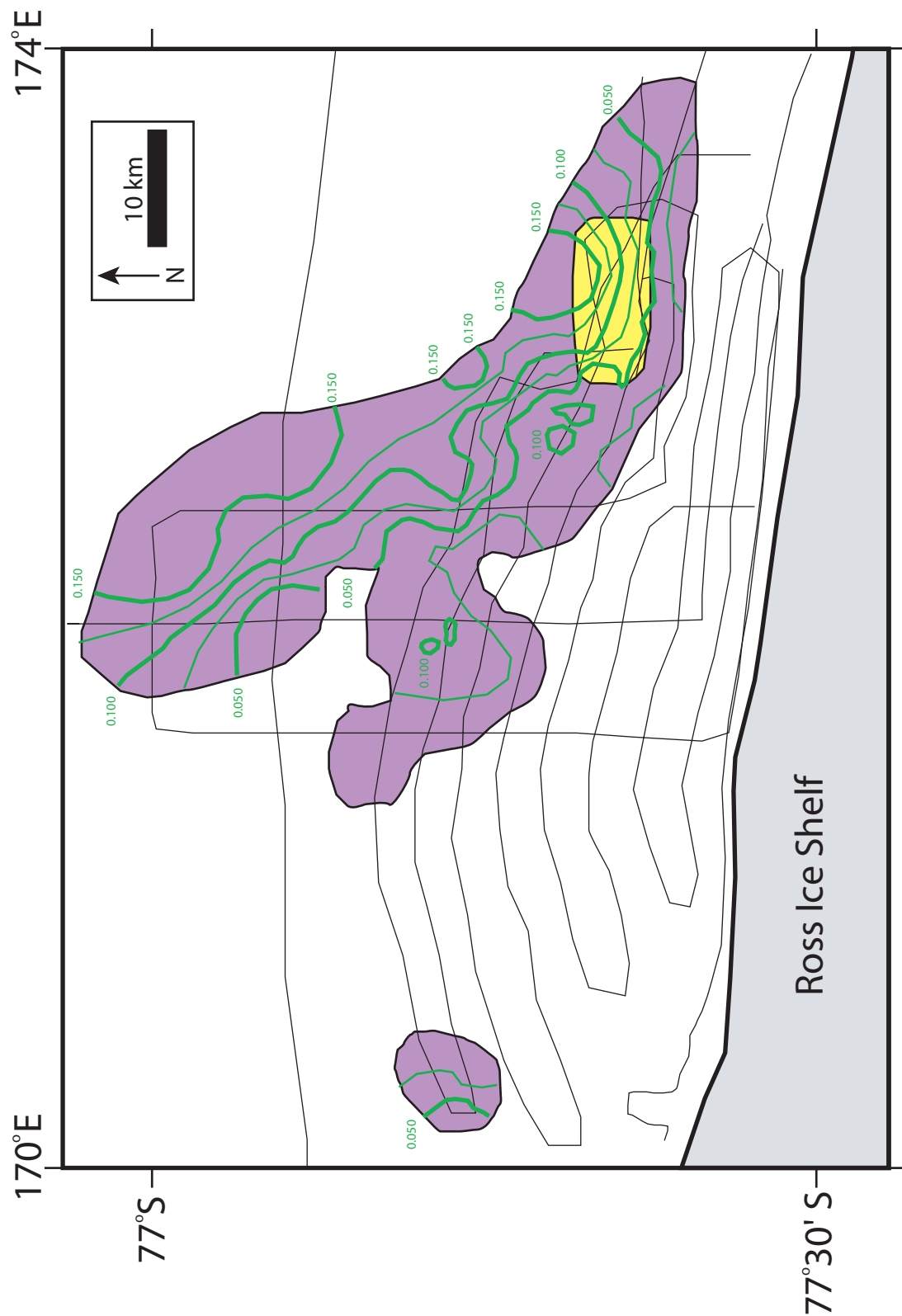


Figure 4.5 - Facies map of unit RSS-4 showing location of mostly reflection free strata (purple) and cross-cutting strata (yellow). Thickness of unit contoured (interval = 0.025 ms).

The interpretation for these two seismic facies is the same as those of unit RSS-3. The near reflection-free areas indicate overcompaction or massive deposition in a sub-glacial environment and the laterally truncated units of the cross-cutting facies suggest sub-glacial cut and fill (Figure 4.3).

4.3 EAIS Evolution

The examination of the seismic stratigraphy of the C-19 site on the Ross Sea continental shelf yields evidence for past ice sheet grounding events. The very first unequivocal evidence for grounded ice is the early Miocene regional uniformity, RSU-5, that is seen throughout the study site. The underlying strata exhibit characteristics that indicate the ice sheet approached but never reached the site at least ten times during the deposition of unit RSS-2, likely spanning the early to late Oligocene. These advance and retreat cycles have never before been seen in seismic data from the Ross Sea.

Units RSS-3 and RSS-4 display similar glacial seismic characteristics. The reflection-free and trough cross-cutting seismic features in these units indicate at least two major ice sheet grounding events on the continental shelf from the early to middle Miocene. Each of these events is represented by a regional unconformity and overlying reflection-free and trough cross-cutting strata (Figure 4.6). While there are many individual cross-cutting troughs within this area, each group is interpreted as a single grounding event because the unconformities are localized and do not fit the regional grounding model. The change from nearly reflection-free to cross-cutting reflections in each of these happens in the same location within the study site (Figures 4.4, 4.5, 4.6). This similarity in depositional styles suggests that ice sheet behavior was similar during each of these grounding events.

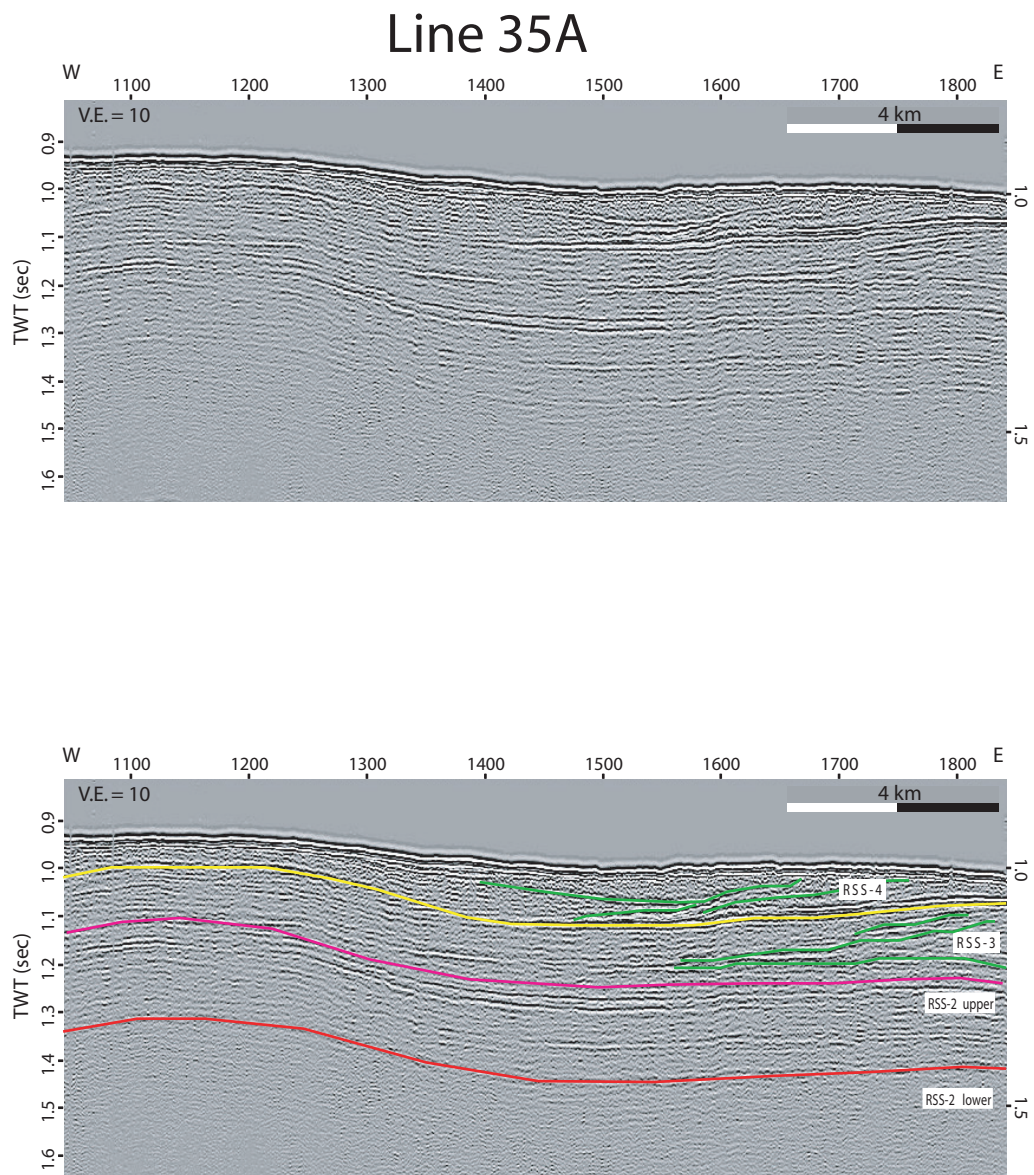
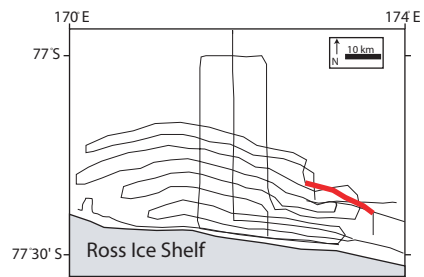


Figure 4.6 - Uninterpreted (top) and interpreted (bottom) seismic line showing cross-cutting reflections of unit RSS-3 and RSS-4 (green lines). Location of line is indicated on lower map.



Various oxygen isotope reconstructions indicate a build-up of ice on Antarctica in the Oligocene (Miller et al., 2005; Shackleton and Kennett, 1975). The direct evidence offered by the stratigraphy of site C-19 indicates that ice did not build-up in large enough volumes to expand onto the continental margin and ground at the C-19 site during this time. The data from the drill sites of western McMurdo Sound, CRP and CIROS, provide definitive evidence for the presence of ice on the Antarctic continental margin in the Oligocene, but it is unclear whether this represents a shelf wide grounding event or local alpine glacier from the Transantarctic Mountains. The seismic stratigraphic evidence from the C-19 study area presents a picture of an ice-free continental shelf during this time, suggesting the data from the CRP and CIROS drill sites represents local glacial activity.

The evidence for grounded ice during the early Miocene from site C-19 does support claims of a large build-up of ice at this time. Miller et al. (1991) identified a cooling event dubbed Mi1 (circa 23.5 Ma) which is consistent with the stratigraphy of C-19. Anderson and Bartek (1992) also offer evidence supporting early Miocene grounding events in the form of large glacially carved troughs on the continental shelf. Massive diamictites recovered at the DSDP sites date back to the late Oligocene-early Miocene, but it is unclear whether they represent subglacial or glacial-marine activity (Anderson and Bartek, 1992). C-19 data supports a subglacial interpretation for these sediments because of the definitive evidence of ice sheet grounding at this time.

The up-dip location of site C-19, where older strata is at shallow depth, offers direct evidence of the history of the evolution of the EAIS through a high-resolution data set. The findings of this study constrain some of the data from the various Ross Sea drill sites and address some of the claims made based on these data sets. The findings of this study will

also aid in determining future drill site in the Ross Sea targeting strata that may help to resolve some of the yet unanswered questions about the history of the EAIS.

4.4 MCS Aliasing

A data set containing both SCS and MCS can be invaluable when investigating both shallow stratigraphy and deeper stratigraphy or structural features, but the limitations of each type of seismic data become apparent when making direct comparisons of seismic features. SCS lacks in its ability to penetrate far into the subsurface to image deep strata, but it excels at imaging shallow strata in high-resolution. Conversely, because of the lower frequency content, MCS data is unable to provide the high-resolution needed to image all types of shallow seismic features faithfully.

The differences between SCS and MCS profiles are most easily observed in the following examples. First, the SCS seismic facies of reflection-free and nearly reflection-free (few internal reflections) appear as only reflection-free strata in MCS. While the visual differences between these types of seismic strata may be slight, the implications for interpreting depositional environments are large. In MCS data all of the SCS seismic facies mentioned above appear as reflection-free packages (Figure 3.15). This reduction of multiple types of SCS facies into one MCS facies can make accurate interpretations difficult.

The second example is the reduction of frequency of individual reflections in MCS. This leads to multiple layers of SCS reflections being seen as one reflection in MCS. This phenomenon can make tracing a single reflection difficult in places where this combination of multiple layers has occurred. This problem is more evident in the shallow portions of the seismic profile than it is in the deeper portions (Figure 3.15).

CHAPTER 5

CONCLUSIONS

- The onset of regional EAIS glaciation on the continental shelf at the C-19 site was in the early Miocene. The seismic evidence for this event is a site-wide erosional unconformity with subsequent deposition of mostly reflection-free strata with scattered cross-cutting troughs.
- There were two major regional groundings of the EAIS on the Ross Sea continental shelf in the early to middle Miocene. The glaciogenic seismic features left behind for the second event are very similar to those left by the initial grounding event.
- During the Oligocene, prior to the onset of widespread glaciation from the EAIS on the continental shelf, this area experienced multiple cycles (at least 10) of ice sheet advance and retreat representing an ice sheet that is approaching but not reaching the C-19 study area. These cycles appear in the seismic record as alternating low to high amplitude reflection representing condensed sections deposited during ice-free time and reflection-free layers deposited as ice-distal to ice-proximal strata.
- Comparison studies of SCS and MCS reveal that the lower source signal frequencies are responsible for a decrease in individual reflection frequencies (wider reflections). The phenomenon leads to difficulties in interpretation due to the following changes:
(1) SCS facies such as reflection-free and nearly reflection-free appear as only reflection-free in MCS profiles, and (2) in the shallower portions of MCS profiles the

decrease in frequency of individual reflections causes some layers to be lost as they are consumed by the wider reflections.

REFERENCES

- Anderson, J.B., and Bartek, L.R., 1992. Cenozoic glacial history of the Ross Sea revealed by intermediate resolution seismic reflection data combined with drill site information. *The Antarctic Paleoenvironment: A Perspective on Global Change: Antarctic Research Series*, 56: 231-263.
- Anderson, J.B., 1999, *Antarctic Marine Geology*. Cambridge University Press, New York.
- Arrigo, K.R, and van Dijken, G.L., 2003. Impact of iceberg C-19 on Ross Sea Primary Production. *Geophysical Research Letters*, 30-16.
- Barrett, P.J., 1975. Textural characteristics of Cenozoic preglacial and glacial sediments at Site 270, Ross Sea, Antarctica. In D.E. Hayes and L.A. Frakes, eds., *Initial Reports of the Deep Sea Drilling Project*, vol. 28. U.S. Government Printing Office, Washington, D.C., pp. 757-767.
- Bart, P.J., 2003. Were West Antarctic Ice Sheet grounding events in the Ross Sea a consequence of the East Antarctic Ice Sheet expansion during the middle Miocene?. *Earth and Planetary Science Letters*, 216: 93 – 107.
- Bart, P.J., and Anderson, J.B., 1997. Glacial Unconformities on the Antarctic Continental Margin, an Example from the Antarctic Peninsula. *From Glaciated Continental Margins: An Atlas of Acoustic Imaged*, ed. Davies, T.A., Bell, T., Cooper, A.K., et al., pages 43-45.
- Bartek, L.R., Anderson, J.L.R., and Oneacre, T.A., 1997. Substrate control on distribution of subglacial and glaciomarine seismic facies based on stochastic models of glacial seismic facies deposition on the Ross Sea continental margin, Antarctica. *Marine Geology*, 143: 223-262.
- Cape Roberts Science Team, 1999. *Studies from the Cape Roberts Project, Ross Sea, Antarctica – Initial report on CRP-2/2A*. *Terra Antarctica*, 6, 1-173.
- Chow, J.M., and Bart, P.J., 2003. West Antarctic Ice Sheet grounding events of the Ross Sea outer continental shelf during the middle Miocene. *Paleo. Paleo. Paleo.*, 198: 169-186.
- Cooper, A.K., Barker, P.F., and Brancolini, G., eds., 1995 *Geology and seismic stratigraphy of the Antarctic margin: American Geophysical Union Antarctic Research Series*, v. 68, 301p., atlas, CD-ROM.
- Davey, F.J., Bennett, D.J., and Houtz, R.E. 1982. Sedimentary basins of the Ross Sea, Antarctica. *New Zealand Journal of Geology and Geophysics*, 25 no. 2: 245-255.

- Denton, G.H., Prentice, M.L., and Burckle, L.H., 1991. Cenozoic history of the Antarctic ice sheet. *Geology of Antarctica*, ed. by R.J. Tingey, Oxford University Press, New York: 365-433.
- Donda, F., Brancolini, G., O'Brien, P.E., De Santis, L., Escutia, C., 2007. Sedimentary processes in the Wilkes Land margin: a record of the Cenozoic East Antarctic Ice Sheet evolution. *Journal of the Geological Society, London*, 164: 243 – 256.
- Hambrey, M.J., Barrett, P.J., and Robinson, P.H., 1989. Stratigraphy. Antarctic Cenozoic history from the CIROS-1 drillhole, McMurdo Sound, ed. by P.J. Barrett, *DSIR Bulletin* 245: 23-48.
- Hambrey, M.J. and Barrett, P.J., 1993. Cenozoic Sedimentary and Climatic Record, Ross Sea Region, Antarctica. *Antarctic Research Series*, 60: 91 – 124.
- Harwood, D.M., and Webb, P.N., 1998. Glacial Transport of Diatoms in the Antarctic Sirius Group: Pliocene Refrigerator. *GSA Today*, 8 no.4: 1-8.
- Haq, B.L., Hardenbol, J., and Vail, P.R., 1987. Chronology of fluctuating sea levels since the Triassic. *Science*, 235: 1156-1167.
- Hayes, D.E., Frakes, L.A., Barrett, P.J., et al., 1975. Initial Reports of the Deep Sea Drilling Project. US Government Printing Office, Washington DC, 28: 1017.
- Holtedahl, O., 1929. On the geology and physiography of some Antarctic and sub-Antarctic islands. *Scientific Results of the Norwegian Antarctic Expeditions, 1927-1928 and 1928-1929*, 172 pp.
- Hughes, T., 1981. Numerical reconstruction of paleo-ice sheets. In G. H. Denton and T. J. Hughes, eds., *The Last Great Ice Sheets*. John Wiley and Sons, New York, pp. 221-261.
- Leckie, R.M. and Webb, P.N., 1986. Late Paleogene and early Neogene foraminifers of Deep Sea Drilling Project Site 270, Ross Sea, Antarctica. *Initial Reports of the Deep Sea Drilling Project*, 90, no. Part 2: 1093-1142.
- Miller, K.G., Wright, J.D., Fairbanks, R.G., 1991. Unlocking the Ice House: Oligocene-Miocene Oxygen Isotopes, Eustasy, and Margin Erosion. *Journal of Geophysical Research*, 96 no. B4, 6829 – 6848.
- Miller, K.G., Wright, J.D., and Browning, J.V., 2005. Visions of ice sheets in a greenhouse world. *Marine Geology*, 217: 215-231.
- Naish, T.R., Woolfe, K.J., Barrett, P.J., Wilson, G.S., Atkins, C., et al., 2001. Orbitally induced oscillations in the East Antarctic Ice Sheet at the Oligocene/Miocene boundary. *Nature*, 413: 719-723.

- Naish, T.R., Wilson, G.S., Dunbar, G.B., Barrett, P.J., 2008. Constraining the amplitude of late Oligocene bathymetric changes in western Ross Sea during orbitally-induced oscillations in the East Antarctic ice sheet; (2) Implications for global sea-level changes. *Paleogeography, Paleoclimatology, Paleoecology*, 260 no.1-2: 66-76.
- Sahagian, D., 1987. Epeirogeny and eustatic sea level changes as inferred from Cretaceous shoreline deposits; applications to the Central and Western United States. *Journal of Geophysical Research*, 92, no. B6, p. 4895-4904.
- Shackleton, N.J. and Kennett, J.P., 1975. Paleotemperature history of the Cenozoic and the initiation of Antarctic glaciation: oxygen and carbon analysis in DSDP sites 277, 279 and 281. Initial Report Deep Sea Drilling Project 29, 743-755.
- Stroeven, A.P., Burckle, L.H., Kleman, J., and Prentice, M.L., 1998. Atmospheric Transport of Diatoms in the Antarctic Sirius Group: Pliocene Deep Freeze. *GSA Today*, 8 no. 4: 1-5.
- Vail, P.R., 1987. Seismic stratigraphy interpretation procedure, *in* Bally, A.W. (ed.), *Atlas of seismic stratigraphy*. AAPG Studies in Geology No. 27, v. 1, p. 1-10.
- VanWagoner, J.C., Posamentier, H.W., Mitchum, R.M., Vail, P.R., et al., 1988. An overview of the fundamentals of sequence stratigraphy and key definitions in C.K. Wilgus, B.S. Hastings, C.G.St.C. Kendall, H.W. Posamentier, C.A. Ross, J.C. Van Wagoner, eds., *Sea-level changes: an integrated approach*. Society of Economic Paleontologists and Mineralogists Special Publication No. 42, p. 39-45.
- Zachos, J., Pagani, M., Sloan, L., Thomas, E., and Billups, K., 2001. Trends, Rhythms, and Aberrations in Global Climate 65 Ma to Present. *Science*, 292: 686 – 693.